THE UNIVERSITY OF MICHIGAN

INDUSTRY PROGRAM OF THE COLLEGE OF ENGINEERING

LABORATORY TECHNIQUES FOR THE DESIGN AND EVALUATION OF AUTOMATIC SYSTEMS TO ALLEVIATE AIRCRAFT RESPONSE TO ROUGH AIR

Rollin G. Lemm

This report is submitted in partial fulfillment of the requirements of The University of Michigan Rackham School of Graduate Studies for the Professional Degree (Aeronautical Engineer) 1960

March, 1960

IP-427

TABLE OF CONTENTS

	Page
LIST OF FIGURES	iii
LIST OF SYMBOLS	v
SUMMARY	1
INTRODUCTION	2
HISTORICAL REVIEW	4
Alleviation Techniques	4
Theoretical Analyses	4
Experimental Studies	16
PROPOSED TECHNIQUE	23
Theory	23
Experimental Procedure	25
Model	26
Instrumentation	30
Disturbance Generator	46
Results	48
Conclusions and Recommendations	57
APPENDIX A - Estimate of Gust Input	59
APPENDIX B - Determination of Pitch Damping	65
REFERENCES	73

LIST OF FIGURES

Figure		Page
1	Block Diagram of Alleviation Scheme	3
2	Problem Formulation	24
3	Coordinate System	28
4	Model Configuration	32
5	Model - Canard Configuration	33
6	Model - Conventional Configuration	34
7	Limits of c.g. Travel in Relation to Wing Aerodynamic Center	35
8	Model Suspension Systems	36
9	Dynamic Suspension System	37
10	Dynamic Suspension System Installed in Wind Tunnel	38
11	Fixed Mount and Balance	40
12	Fixed Mount Installed in Wind Tunnel	41
13	Model Mounted on Balance System	42
14	Block Diagram of Flap Controls	43
15	Flap Control Servomechanism	44
16	Elevator Control Servomechanism	45
17	Disturbance Generator	47
18	Bump Position vs. Time	49
19	Fixed Mount Calibration Curves	50
20	C_N vs. α for Various δ_f	51
21	$C_{M_{c.g.}}$ vs. α for Various δ_f	52
22	C_N vs. α for Various δ_e	53
23	$C_{M_{c.g.}}$ vs. α for Various δ_e	54

Figure		Page
24	C_N and $C_{M_{cg.}}$ vs. δ_f for $\alpha = 6°$	55
25	C_N and $C_{M_{cg.}}$ vs. δ_e for $\alpha = 4, 6, 8°$	56
26	Controls Phase Shift Variation with Forcing Frequency	58
A-1	Model-Bump Orientation and Variation of α Due to Bump	60
A-2	Airplane in Non-uniform Stream	62
A-3	5 x 7 Tunnel Flow Inclination	63
B-1	Model Mounting for Damping Tests	66
B-2	Instrumentation for Damping Tests	68
B-3	Pitch Damping Data (V = o)	69
B-4	Pitch Damping Data	70

LIST OF SYMBOLS

a_1	angle of attack at airfoil leading edge with bump at ℓ_1
a_2	" " " " " " " ℓ_2
A.C.	aerodynamic center of wing
AR	aspect ratio of wing
AR_t	" " tail
a_n	normal acceleration
b	wing span
c	wing mean aerodynamic chord
c.g.	center of gravity
C_L	lift coefficient
C_M	moment coefficient
c_l	sectional lift coefficient
$c_{M_{c/2}}$	" moment coefficient aboud mid-chord
c_p	pressure coefficient $= \frac{p - p_\infty}{q_\infty}$
d	differential operator
D	" " " -- denotes differentiation with respect to time
D'	non-dimension form of D, $= \frac{D}{V_\infty/c}$
e	base of natural logarithms
f_n	natural frequency $= \frac{\omega'}{2\pi} \frac{V_\infty}{c}$
I_{yy}	moment of inertia about the c.g.
k	spring constant
k_y	radius of gyration about the c.g.
k'_y	non-dimensional form of k_y, $= \frac{k_y}{c}$
ℓ	tail length
ℓ_o	zero position of bump

l_1 maximum downstream bump position

l_2 " upstream " "

L dynamic lift or scale of turbulence

L_{ij} differential coefficients of equation of motion

L_q quasi-steady lift

m lift curve slope of wing

m_t " " " tail

m_o lift curve slope of an infinite wing

m_1 slope of α vs. ξ/c plot with bump at l_1

m_2 " " " " " "l_2

M mass of airplane

$N.P.$ neutral point

p pressure

q pitching rate

$\bar{q}$ dynamic pressure

S wing area

s distance traveled in time t in half chord lengths = $\frac{2Vt}{c}$

S_t tail area

S_{ij} differential coefficients of equations of motion

t time

t' non-dimensional time = $\frac{tV_o}{c}$

T_n transfer functions

$T(i\omega)$ airplane admittance

u perturbation velocity in x- direction

u_r " " " radial direction

u_θ " " angular velocity

v " " Velocity in y - direction

V velocity

W airplane weight or weighting function

W/S wing loading

w plunging velocity

x distance along chord from mid-chord (also used as upstream direction in wind-tunnel coordinates -- see Figure 3)

x/c static margin

y direction normal to airfoil (also used as direction perpendicular to the x, z plane in wind tunnel coordinates)

$y(t)$ system output

z vertical displacement in wind tunnel coordinates

$\dot{z}'$ non-dimensional plunging velocity = $\dot{z}/V_\infty$

α angle of attack of airplane

α_o trim " " "

α_1 angle of attack on airfoil with bump at ℓ_1

α_2 " " " " " " ℓ_2

β scale factor

γ flight path angle

Γ_φ quasi-steady circulation

δ control deflection

δ_α change in α due to motion of bump

$\delta_{\alpha_{eq}}$ equivalent uniform angle of attack

θ pitch angle

$\bar{\theta}$ angle used in polar representation of x

μ, η non-dimensional mass = $\frac{2M}{\rho S c}$

ξ position from leading edge of airfoil

ρ air density

Σ summation

ϕ velocity potential, Wagner function, or correlation function

Φ power spectral density function

Ψ stream function

Ψ Kussner function

σ standard deviation

ω circular frequency

Superscripts and subscripts:

$\overline{(\ )}$ refers to surface values

$\dot{(\ )}$ denotes time differentiation

$(\ )_\alpha$ denotes differentiation with respect to α

$(\ )_q$ " " " " " q

$(\ )_m$ refers to model

$(\ )_p$ refers to prototype

$(\ )_\infty$ refers to free stream conditions

$(\ )_e$ refers to elevator

$(\ )_f$ refers to flap

$(\ )_o$ refers to initial values

Additional definitions are given as symbols are introduced.

SUMMARY

The purpose of this study is to develop laboratory techniques for the implementation of a new approach to the problem of alleviation of airplane response to rough air. The literature reporting the results of previous investigations of the response alleviation are reviewed and summarized. The theoretical considerations of the new approach are discussed briefly, and the test program to obtain the required experimental data is outlined. A dynamically scaled model airplane is designed to be used in conducting the test program. Servo systems are designed to operate the movable control surfaces in the model in response to electrical input signals. A two-component balance system and a dynamic suspension system with two degrees of freedom are also designed. The portions of the outlined test program defining the static and dynamic characteristics of the model are completed, and unsteady aerodynamic effects also are evaluated. A method of obtaining sustained oscillations of a moving-bump type gust generator is developed to simulate sinusoidal atmospheric disturbances in a wind tunnel.

The components which are designed and tested generally are found to operate satisfactorily. Some modifications to the dynamic suspension system are suggested to improve its operation. The development and tests were conducted at the University of Michigan under the supervision of Professor J. D. Schetzer. The tests were conducted in the 5' x 7' low-speed, low-turbulence wind tunnel at the University's Aeronautical Engineering Laboratory.

INTRODUCTION

Since the late 1930's, various attempts have been made to develop effective devices to alleviate the response of airplanes to rough air. These attempts consist of both analytical and experimental investigations. The literature reporting the results of these studies is reviewed and discussed. These previous efforts are found to have resulted in alleviation systems which are "closed loop" in nature in that the aircraft motion is fed back to the control system by the aerodynamic effects. Hence, the systems are limited in effectiveness by the dynamic instability which naturally arises. A study [41] was undertaken at the University of Michigan to explore the possibility of circumventing the instability problem by devising a gust-sensing mechanism that is nearly independent of the control measures used to alleviate the gust response. In such a system, the gust input alone commands the control output and the system responds in an "open loop" manner. The general alleviation problem is resolved into two parts in the "open loop" approach. The first part involves the programming of the gust input to the controls such that the gust is cancelled as nearly as possible. The programming is designed to provide cancellation in the critical frequency range which is determined by the input spectrum and the natural frequency of the airplane. The second part of the problem involves making the gust sensor independent of the airplane motion. The gust is sensed by means of an auxiliary airfoil or vane, and the effects of motion of the airplane are removed by adding signals from pitch and plunge sensors directly to the control surfaces. A block diagram of the alleviation scheme is shown in Figure 1.

The implementation of the "open loop" approach to alleviator design requires certain physical data which can best be obtained by experimentation. A test program has been outlined [41] to provide the required data. The reported study was concerned with the development of laboratory techniques to carry out the test program to obtain the necessary data.

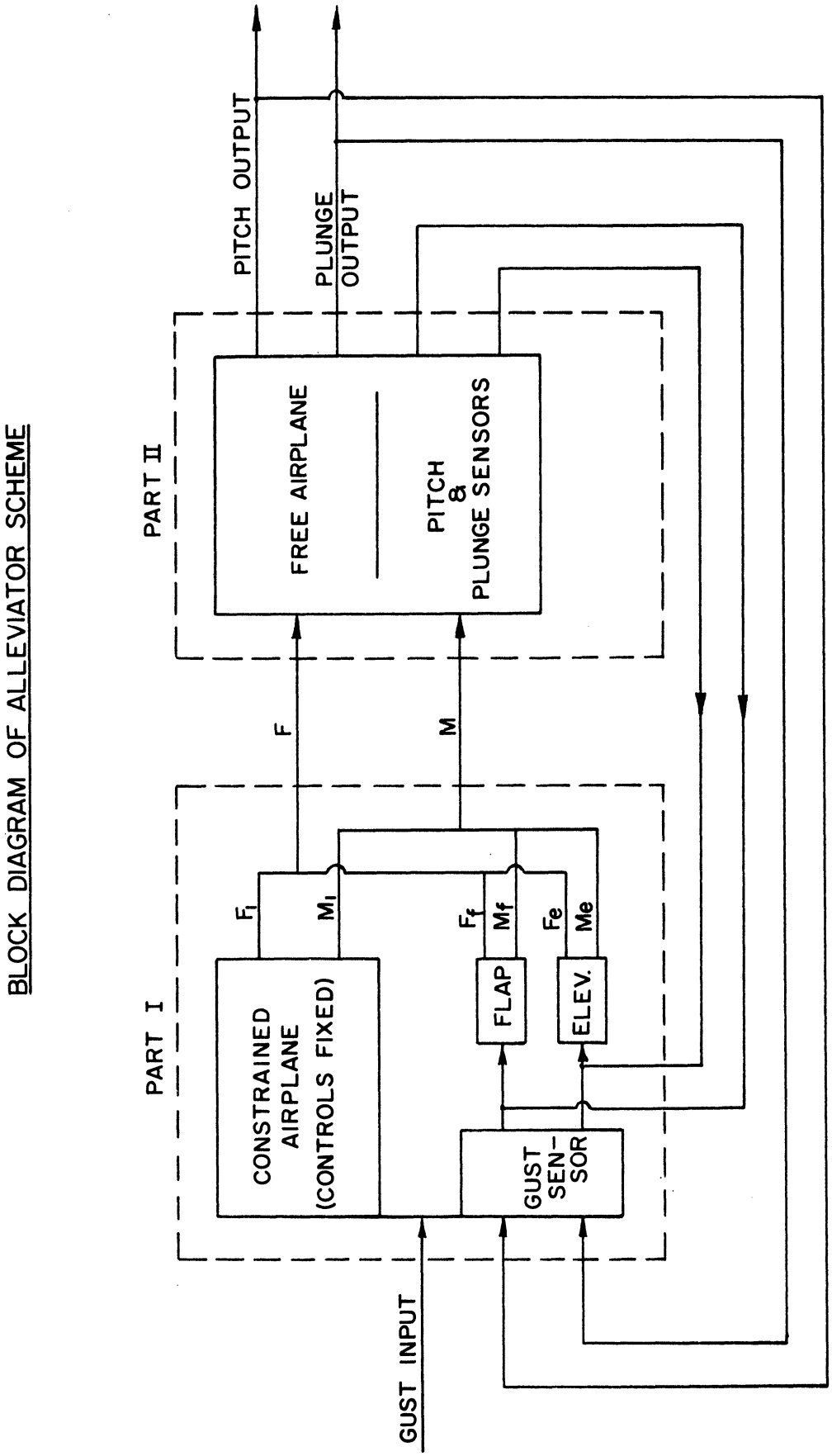

Figure 1. Block Diagram of Alleviation Scheme.

HISTORICAL REVIEW

Alleviation Techniques

Most schemes for alleviation of the response of aircraft to rough air disturbances obtain the alleviation by structural deformation or operation of control surfaces, or both. Alleviation systems using structural twist and bending of the wing are reported by Shufflebarger[1] and Reisert[2]. Hirsch[3] and many NACA researchers investigated various means of using control surfaces as alleviation devices. A combination of wing bending and flap deflection was proposed and tested by Douglas Aircraft Company[4].

The theoretical and experimental procedures which are employed in these investigations are discussed in the following paragraphs.

Theoretical Analyses

Three fundamental theoretical methods are used to analyze the response of aircraft to atmospheric disturbances. These are the Stability Derivative Analysis, the Superposition of Elemental Solutions, and the Generalized Harmonic Analysis.

In the Stability Derivative Analysis, the dynamic stability and response of rigid body aircraft is described by a set of non-linear differential equations of motion[5]. Stability and response to atmospheric conditions and disturbances are analyzed ordinarily in terms of small motions from a steady-state condition; therefore, the set of equations can be linearized and, due to the airplane symmetry, analyzed as two independent sets of equations. The longitudinal oscillations of concern in dynamic stability and response at moderate airplane speeds are of small frequency[6] and, therefore, the aerodynamic constants are assumed to be independent of frequency in many early analyses. The aerodynamic constants are then derived from time-varying boundary conditions using steady flow theory. Later studies add correction terms to account for the finite time for wing vorticity to reach the tail. The above considerations lead to the assumption that the aerodynamic reactions to the airplane motion depend only on position and velocity, and not upon higher time derivatives or integrals of the motion. Assuming the forces and moments to be linearly dependent on their respective variables, the second and higher degree terms may be dropped and the equations written as first degree differential equations. As an example, the equation defining the change in pitching moment following a small displacement is written by Tobak[6] as follows:

$$\frac{I}{\bar{q}_\infty S c}\ddot{\alpha} = \left(\frac{\partial C_M}{\partial \alpha}\right)\alpha + \left[\frac{\partial C_M}{\partial(\dot{\alpha}c/2V_\infty)}\right]\frac{\dot{\alpha}c}{2V_\infty} + \left[\frac{\partial C_M}{\partial(\bar{q}c/2V_\infty)}\right]\frac{\dot{\alpha}c}{2V_\infty}$$

The partial derivative coefficients may be treated as constants under the above assumptions; hence, the equations are linear, second order, differential equations with constant coefficients. The coefficients are termed stability derivatives; hence, the name of the analysis.

The systems of linear, differential equations thus derived may be solved by any of the standard methods of analysis available for the solution of such equations. Operational calculus methods are particularly well suited to the solution of such systems of equations with arbitrary forcing functions. Three such methods are the Fourier transform, Laplace transform, and the Impulse Method. The first two of these operational mathematical methods transform functions of time into frequency functions which are summed over all frequencies to obtain time functions representing the system response. The Impulse Method remains entirely within the time domain and uses the superposition integral to obtain the system response to arbitrary forcing functions. The response of the system to the unit impulse at a time τ is summed by convolution over all values of τ. This unit impulse response is called the weighting function, and is an elementary solution for the system. Hence, the Impulse Method may be considered to be one form of the second fundamental method of analysis.

The superposition integral is used in the Method of Superposition of Elemental Solutions to write the equations of motion. Elemental force and moment functions are superimposed and equated to the inertial forces and moments in accordance with Newton's second law. The indicial aerodynamic functions defined by Tobak[6] as the aerodynamic response of the airplane as "functions of time to instantaneous change in one of the conditions determining the aerodynamic properties of the airplane in steady flow", are a type of elemental solution. The expressions for the indicial functions are obtained by use of linearized, unsteady aerodynamic theory. Such functions were first derived by Wagner[7] for the two-dimensional wing in incompressible flow, and have since been obtained by Heaslet[17] and Lomax[18] for subsonic and supersonic compressible flow. An example of one of the equations of motion written by the above procedure by Tobak[14] is as follows:

$$\eta \gamma'(\phi) = \frac{d}{d\phi}\int_0^{\phi} C_{L_\alpha}(\xi)\,\alpha(\phi-\xi)\,d\xi + \frac{d}{d\phi}\int_0^{\phi} C_{L_q}(\xi)\,q(\phi-\xi)\,d\xi + l\alpha_g\, C_{L_g}(\phi)$$

where
- η = dimensionless mass parameter = $MV^2/q_\infty Sc$
- γ = flight path angle
- ϕ = chord lengths of travel in time t_1 = Vt/c
- ξ = variable of integration
- α = angle of attack
- $l\alpha_g$ = step change in dimensionless gust velocity = w_g/V
- $C_{L_\alpha}(\phi)$ = indicial lift response to unit step change in α
- $C_{L_q}(\phi)$ = " " " " " q
- $C_{L_g}(\phi)$ = " " " " " w_g
- q = dimensionless pitching velocity = $\frac{\dot{\theta}c}{V}$

A system of linear equations defining the response of the airplane in the degrees of freedom considered is written as indicated in the above example. This system is then solved for the variable of interest by standard methods of solution of linear differential equations. A convenient means of solution of the system is by the use of Laplace transforms. The system of equations developed as outlined above is exact (within the limitations of linearized theory) with complex expressions for the indicial functions. The solution of the system in its exact form is a formidable task; consequently, various approximations have been introduced to simplify the problem. Some of the more basic of these approximations are mentioned briefly below:

The exact mathematical expressions for the indicial functions are not expressible in terms suitable for analytical studies; therefore, approximate expression such as the Wagner or Kussner[7] functions are usually substituted. Wagner's approximation is a function which defines the response of a rigid airfoil to a step change in angle of attack as the ratio of the lift at any instant to the steady-state lift.

$$\phi(s) = 1 - 0.165\, e^{-0.0455 s} - 0.335\, e^{-0.3 s}$$

where $s = \frac{2V}{c} t$ = distance traveled relative to the free stream in half-chords.

The Kussner function has a definition analogous to that of the Wagner function, but is in response to the penetration of a sharp-edged gust. The approximation for this function as derived by Sears and Sparks[9] is

$$\psi(s) = 1 - 0.5\, e^{-0.13 s} - 0.5\, e^{-s}$$

where s is defined as before.

Another approximation frequently used consists of replacing the indicial lift and moment functions by their steady-state values, i.e., replace $C_{L_\alpha}(\phi)$ by $C_{L_\alpha}(\infty)$, etc. These steady-state terms are the stability derivatives. A further simplification frequently made is the replacement of the indicial gust functions by constants equal to their respective steady-state values, i.e., replace $C_{L_g}(\phi)$ by $C_{L_g}(\infty)$, etc.

Analyses are often made in which the pitching degree of freedom is neglected. This approximation reduces the degree of the characteristic equation, thereby simplifying the solution of the system. Another common practice is to consider forces and moments due to loads on wing and tail only.

The response of an airfoil to an arbitrary atmospheric disturbance may also be obtained by the superposition of another type of elementary response function -- the Sears function for a sinusoidal gust. The lift and moment per unit span experienced by a rigid airfoil on passing through a sinusoidal gust of reduced frequency ω are found by Sears[9] to be expressible as

$$L = \pi \rho c U W e^{ivt} \frac{J_0(\omega) K_1(i\omega) + i J_1(\omega) K_0(i\omega)}{K_1(i\omega) + K_0(i\omega)}$$

$$M_{1/2} = Lc/4$$

where
ρ = density
c = chord length
U = velocity passing through gust
W = max. amplitude of gust
v = frequency of waves passing
ω = reduced frequency = $vc/2U$
$J_n(\omega)$ = Bessel functions of the first kind, order n
$K_n(i\omega)$ = " " " second " " n

Defining the Sears function as $\phi(\omega)$, the expressions for lift and moment per unit span become

$$L = \pi \rho c U W e^{ivt} \phi(\omega)$$

$$M_{\frac{1}{2}} = \pi \rho \frac{c^2}{4} U W e^{ivt} \phi(\omega)$$

where $\phi(\omega) = \dfrac{J_0(\omega) K_1(i\omega) + i J_1(\omega) K_0(i\omega)}{K_1(i\omega) + K_0(i\omega)}$

The expression for $M_{\frac{1}{2}}$ indicates that the resultant lift acts through the quarter-chord point.

An arbitrary gust profile may be obtained by the superposition of sinusoidal functions; therefore, the forces and moments experienced by the airfoil, due to an arbitrary disturbance, may be obtained by superposition. The forces and movements due to oscillations of the airfoil are neglected and the aerodynamic forces and moments are obtained by superposition using the Fourier integral. The forces and moments thus obtained are then equated to the inertial forces to obtain the equations of motion. The general result is a system of differential equations which may be solved for the airfoil response by standard methods.

The method of superposition of elemental solutions may be applied to obtain the airplane response to arbitrary atmospheric disturbances. However, the method has usually been restricted to the determination of the response to ramp-type disturbances by superposition of indicial

step responses. An exception is a study by Richardson[10] in which indicial impulse responses are superposed to obtain the response to random disturbances, a technique which introduces the third fundamental method of analysis, Generalized Harmonic Analysis.

The response of a linear system to an arbitrary function of time may be expressed by the superposition integral as[5]

$$y(t) = \int_{-\infty}^{t} W(t-\tau) f(\tau)\, d\tau$$

where $W(t-\tau)$ = weighting function of the system
$f(\tau)$ = arbitrary forcing function
τ = variable of integration
$y(t)$ = system response

The weighting function is defined as the response of the system to a unit impulse applied to the system at time $t = \tau$; hence, the weighting function is the indicial impulse function discussed previously. If $f(\tau)$ is a random function, statistical methods must be applied to obtain a stochastic measure of the response. Generalized Harmonic analysis is such a statistical method. In such a case, the response may be written as

$$y(t) = \int_{-\infty}^{\infty} W(t-\tau) f(\tau)\, d\tau = \int_{-\infty}^{\infty} W(\tau) f(t-\tau)\, d\tau$$

where a change of variables has been introduced to obtain the second integral from the first. The response, $y(t)$, is a random function because $f(\tau)$ is a random function. Assuming the forcing function to be a stationary random process, a statistical prediction is possible. A measure of this statistical prediction can be obtained from the relationship between the response at time t with the response at a time $(t + t_1)$. This relationship is indicated by the auto-correlation function, which is defined as follows:

$$\phi_{yy}(t_1) = \overline{y(t)\, y(t+t_1)} = \int_{-\infty}^{\infty}\int_{-\infty}^{\infty} W(\tau) W(\tau')\, \overline{f(t-\tau) f(t+t_1-\tau')}\, d\tau\, d\tau'$$

where the bar indicates the mean value, and the subscript $(\ )_{yy}$ indicates an auto-correlation. The auto-correlation function for $t_1 = 0$ is the mean square value of $y(t)$ and may be used as measure of the response intensity; i.e.,

$$\phi_{yy}(0) = \overline{y^2(t)}$$

Any continuous function, such as $y(t)$, may be considered to be composed of an infinite number of sinusoidal components with frequencies between 0 and ∞. If that portion of $\overline{y^2(t)}$ obtained from components having circular frequencies between ω and $\omega+d\omega$ is denoted by $\Phi(\omega)\,d\omega$, then the mean square value may also be written as

$$\overline{y^2(t)} = \int_0^\infty \Phi(\omega)\,d\omega$$

Since $\overline{y^2(t)}$ is analogous to power, the function $\Phi(\omega)$ is called the power spectral density function.

The power spectral density function is introduced because of a valuable relationship which exists between the power spectra of the system input and output and the system frequency response function. It is possible to show[5] that, for linear systems,

$$\Phi_o(\omega) = \Phi_i(\omega)\,|T(i\omega)|^2$$

where $\Phi_o(\omega)$ = power spectral density of system output
$\Phi_i(\omega)$ = " " " " input
$|T(i\omega)|$ = modulus of the mechanical admittance of the system.

It can also be shown that the power spectral density function is reciprocally related to the auto-correlation function by the Fourier transform. Hence, the input spectral density function may be obtained from an experimentally determined auto-correlation function of the input. The output spectral density function can then be determined, and the mean square value of the system response can be evaluated as

$$\overline{y^2(t)} = \int_0^\infty \Phi_o(\omega)\,d\omega$$

Certain basic assumptions are made in order to apply the power spectral analyses to the determination of airplane response to random atmospheric disturbances. One such assumption is that the atmospheric disturbance is a stationary random process. A stationary random process is one which depends only on the differences in the values of the independent variable (usually time) involved, and for which the statistical parameters remain unchanged for every translation of the independent variable[11]. In gust analyses, the independent variable concerned is time or space. As previously indicated, this assumption allows a statistical prediction of the response of the system to the disturbance. In the large, atmospheric turbulence can be expected to vary with time and space (i.e., from day to day, or between widely separated locations), but the variations are slow enough so that the disturbance can normally be assumed stationary for any given flight.

The disturbance frequently is assumed to be homogeneous or isotropic for the purpose of analysis. A turbulence field is homogeneous if its velocity components are statistically independent of the space coordinates; i.e., the statistical parameters do not change with location in the field[5]. The assumption of homogeneity makes it possible to translate time histories of atmospheric turbulence experienced by an airplane flying through the turbulence into a spatial structure of roughness. An isotropic turbulence field is one in which the statistical properties are independent of reflection or rotation of the coordinate axes. In such a field, the mean square value of the three components of turbulence velocity are equal, and the mean values of all cross products of the components are zero (i.e., $\overline{u^2} = \overline{v^2} = \overline{w^2}$ and $\overline{uv} = \overline{uw} = \overline{vw} = 0$). Flight test results[12] indicate that the assumption of isotropic turbulence may be valid, at least to the extent of two-dimensional (v and w) isotropy.

One may frequently be able to assume the atmospheric turbulence and the airplane response are both normally distributed. As a consequence of the central limit theorem of probability theory[11] and the properties of linear systems, the response may be considered normally distributed if the disturbance is normally distributed. Flight test results tend to verify the validity of the assumption that the disturbance is so distributed[12]. Some of the benefits of making this assumption are, (1) the Gaussian distribution has been widely studied, (2) it may be characterized entirely by its mean square (standard deviation), and (3) the mean-square parameter provides a link between amplitude spectra and power spectra.

Other less basic assumptions are made to simplify specific analytical treatments of the rough air response problem. Some of these assumptions are as follows:

(1) airplane assumed to be a rigid body
(2) consideration of normal velocity components in the vertical plane (w)
(3) consideration of a two-dimensional airfoil
(4) consideration of wing only

Application of Stability Derivative Analysis

An extensive study, based on the stability derivative method of analysis, is reported by Phillips and Kraft[13]. Analyses are made of various systems for increasing the smoothness of flight through rough air. In the systems considered, the wing flaps and elevators are operated automatically in response to the indications of an angle-of-attack vane or an accelerometer. The effectiveness of the alleviation system considered is determined by calculations of the airplane response to steady, sinusoidal atmospheric disturbances. The gust disturbance is assumed to consist of alternate regions of upward and downward vertical velocity in the path of the airplane, and is assumed to be invariant with time and wing span. The response of the basic airplane is obtained for characteristics which are fairly representative of a modern transport flying at sea - level and 200 mph. Various combinations of flaps and elevators are used as control surfaces to obtain the alleviation. Conditions are found under which alleviation may be obtained by the use of flaps alone, without causing pitching, and modifications to standard flaps are suggested which will result in approximate satisfaction of these conditions. Alleviation of the aircraft response to about one-fifth of that of the basic airplane is found to be theoretically obtainable. Stability and control characteristics are found to be satisfactory with suitable choice of parameter values.

The stability derivative analysis is used by Tobak[14] to derive approximate longitudinal responses of a rigid airplane to step and harmonic gusts. These approximate solutions are compared with those of more exact methods to evaluate the validity of the approximations made in the stability derivative analysis. The results of the stability derivative studies are found to provide excellent approximations to the true values for the cases considered.

Boucher and Kraft[15] use the stability derivative approach in an analogue computer simulation of an airplane equipped with a vane-controlled gust-alleviation system. The analysis considers a twin-engine light plane with flaps and elevators modified as suggested by Phillips and Kraft[13]. Refinements are made in the analysis to include downwash lag, servomechanism characteristics, etc. Unsteady aerodynamics are neglected, and constant forward velocity is assumed. Responses to step gusts and control deflections are obtained for an "optimum" alleviation system (i.e., a system such that normal force and moment due to α are zero) and for a system such that the airplane has a small positive static margin. Effective alleviation is obtained, but complete alleviation is not obtained because of lag in servo response.

Applications of the Superposition of Elemental Solutions

Tobak[6] applies the method of Superposition of Elemental Solutions to study the motion of isolated wings and wing-tail combinations. A

single degree of freedom (pitching) is considered; the wing executes a harmonic pitching motion while the c.g. traverses a level path at constant velocity. The aerodynamic forces and moments are functions of the normal velocity which is composed generally of that due to the instantaneous angle-of-attack and that due to the pitching velocity. The lift and moment coefficients are expressed in terms of the superposition of four indicial solution components, C_{L_α}, C_{L_q}, C_{M_α} and C_{M_q}. The four components are found to be frequency dependent functions and to be basically different for subsonic and supersonic speeds. The effect of wing vorticity or wing damping is considered for the wing-tail combination. A simplified supersonic case is considered for wing-tail combinations. Exact solutions for the tail load are obtained for the special case of a yawed triangular wing in a supersonic stream by use of strip theory, and the results are compared with those obtained by superposition of the gust function used in gust analyses. Gust analyses results are found to be suitable. The results are applied to the dynamic stability analysis of the single degree-of-freedom case in rotary oscillation. A comparison is made to evaluate the choice of an "effective tail length" used in the usual dynamic stability analyses. This choice is found to be surprisingly accurate.

Tobak[14] also uses the Superposition of Elemental Solutions in a study to obtain the response of an airplane to step and harmonic gusts. Two degrees of freedom are considered (pitch and plunge) and the equations of motion are written, using the superposition of indicial solutions which are assumed known. The resulting equations are solved, using Laplace transform theory. Numerical calculations for the step and harmonic gust responses are obtained for a rectangular wing of aspect ratio 3 flying at Mach 1.2, and comparisons are made with results obtained by the Stability Derivative Analysis.

Reisert[2] and Croom[16] apply the Superposition of Elemental Solutions to determine the responses of model airplanes to ramp gusts from experimentally determined step-gust responses. Donely and Shufflebarger[19] study the effectiveness of a dynamically overbalanced flap as a gust alleviator by the superposition method of analysis.

Application of Generalized Harmonic Analysis

One of the first applications of the generalized harmonic theory of communications to problems of airplane dynamics is that made by Liepmann[20]. The theory is applied to determine the response of a linear, second-order system to a random forcing function. The relationship between the input and output power density spectra is derived for a random forcing function, and an expression is obtained for the mean-square displacement of the system. Liepmann applies the results to a two-dimensional airfoil in incompressible, turbulent flow to obtain an expression for the mean square lift coefficient. The mean-square lift coefficient is obtained in terms of the normal velocity component and the turbulence scale by using an assumed

form for the power spectral density of atmospheric turbulence. The lift due to large scale turbulence over a wing of small chord is shown to be the same as obtained by quasi-steady theory. The mean-square lift due to small scale turbulence over a large wing is shown to be negligible. The probability and frequency of obtaining excessive values of the response are evaluated.

The statistical approach to the buffeting and gust response problem is extended by Liepmann[21] to include wings of finite span. The finite span airfoil is replaced by finite span lifting line in a free stream moving with a constant velocity. An integral expression is obtained for the mean-square lift in terms of the input power spectral density and the admittance of the wing. Three limiting cases are considered; (1) the two-dimensional case with three-dimensional velocity fluctuations, (2) indicial response to a step change in α independent of span, and the turbulence assumed isotropic and homogeneous; and (3) the turbulence spectrum assumed to be the same as used previously[14]. Expressions are obtained for the mean-square lift coefficient in each case in terms of the wing admittance and the input power spectra.

Press, Mazelsky and Houbolt[22, 23] report studies of applications of generalized harmonic to gust loads on airplanes. The basic concepts of the theory are reviewed and the normal acceleration of the airplanes due to gusts are obtained in terms of the input power spectral densities and the airplane admittances. The normal acceleration increment is assumed to be normally distributed with zero mean, and the standard deviation of the normal acceleration is shown to be a useful measure of the intensity of the applied load. The power spectral density of the normal acceleration is obtained from the input power spectrum and the airplane admittance. The airplane admittance is obtained by integrating the airplane response to a step gust. The step gust response is assumed to be defined by the Kussner function up to the response peak, and by the airplane dynamic characteristics thereafter. The admittance is found to be very sensitive to changes in aerodynamic damping; hence, the airplane short-period characteristics are found to have an appreciable effect on gust loads. A numerical procedure for the estimation of power spectra, based on results by Tukey[24], is outlined by Press and Houbolt[23]. Criteria for the design of experiments for spectra determination are outlined. The effects of c.g. position, low short-period damping, and wing-bending flexibility on aircraft gust loads are studied. A rearward shift of c.g. position is found to cause a shift of the power spectrum peak to a lower frequency and to increase the magnitude of the peak. Low, short-period damping and a high degree of wing flexibility are found to seriously amplify gust loads in rough air.

Richardson[10] extends the concepts introduced by Liepmann to include the complication introduced by a multiple degree-of-freedom system. The analysis includes the three rigid-body degrees of freedom (plunging, pitching,

and rolling), and an unspecified number of elastic degrees of freedom. The equations of motion are written, using Lagrange's equation, in a matrix notation with coordinates for plunge (z), pitch (θ), roll (ϕ), and elasticity (ξ_r). The equations are solved for acceleration of the airplane c.g. and wing root bending moment in response to random forcing functions. The auto-correlation function of the normal acceleration is obtained, assuming the forcing functions to be stationary, random functions. Numerical solutions are given for some simple examples with a one-dimensional gust structure. Unsteady aerodynamic effects are found to be small for turbulence with a scale large compared to the wing chord. Large values of the relative density of the airplane are found to further decrease the importance of unsteady aerodynamics, and to decrease the importance of the pitching degree of freedom. The pitching degree of freedom is found to become increasingly important as the scale of turbulence increases.

Diederich and Drischler[25] present an analysis which parallels, to some extent, that of Richardson. The purpose of the analysis is to determine the effect of spanwise variation in gust intensity on the lift due to atmospheric turbulence. The lift spectra and correlation functions are obtained for several spanwise weighting functions and various atmospheric spectra. These calculations are made for both the normal and longitudinal components of turbulence which are assumed to be stationary and isotropic. An "average" gust power spectral density is defined as an approximate method of considering the spanwise variations in gust intensity. The power spectral density of the lift due to the normal turbulence component is written in terms of this "average" spectral density and the admittance of the system. A similar expression is obtained for the lift due to the longitudinal turbulence component, but no such "averaging" technique is available in this case. The power spectrum of the total lift is obtained by superposition of the component spectra. Six special cases are considered and the calculated spectra are found to agree closely with experimental data. The changes in mean-square normal velocity, due to the spanwise load variations, are small for small values of the ratio of span to the scale of longitudinal turbulence.

A recent theoretical analysis which considers the response of a complete airplane to flight-through-random turbulence is presented by Etkin[26]. The four elements of the problem, as considered by Etkin, are (1) the statistical description of the turbulent field, (2) the calculation of the aerodynamic forces and moments due to the field, (3) the calculation of the transfer functions, and (4) the combination of the input and transfer functions to obtain the output. The analysis considers one elastic and five rigid-body degrees of freedom. Spanwise gust variations are considered. The turbulence is represented as the superposition of sinusoidal waves of shearing motion, as suggested by Ribner[27]. Only the vertical gust component is considered. The turbulence waves, which are generally inclined with respect to the airplane plane of symmetry, are resolved

into components along the body axes. The turbulent field is assumed stationary and isotropic. The mean square gust velocity is written as the double integral of the two-dimensional power density spectrum of the turbulence. The integration variables are the two wave numbers of the turbulence components. The power density spectrum of the turbulence is assumed to be of the same form as applies to wind-tunnel tests. The resultant two-dimensional spectrum is integrated with respect to the wave number of the lateral turbulence component to obtain a one-dimensional power density spectrum. Each spectral component of the gust velocity is approximated by a modified two-dimensional Taylor's series in which each term describes a certain periodic rigid or elastic motion. All turbulence components having wave lengths of less than two chord lengths are neglected. An error analysis indicates that the approximations are acceptable. The relationships between forces and moments are expressed in matrix notation and the lateral and longitudinal motions are separated. The transfer functions relating the unknown variables to the mean gust velocity are calculated from the inverse characteristic matrix and the forcing matrices. The mean-square response is formulated from the transfer functions and the input power density spectra. The author calculates the normal force coefficient and moment coefficient for a flat-plate, two-dimensional airfoil and compares the results with Sear's exact solutions as a check on the approximations involved in the analysis. The errors are found to be small.

Another aspect of communication theory, Weiner's optimum filter theory, is applied to the gust alleviation problem by Tobak[14]. The particular problem considered is the design of a vane-controlled alleviation system which minimizes the deviation of the airplane from a straight and level flight path with no pitching. The degrees of freedom considered are the normal acceleration and the pitch rate. It is assumed that (1) the control system commands result in independent forces and moments on the airplane, (2) the statistical nature of the gust is known, and (3) the indicial lift and moments due to gust and control deflections are known. Two equations of motion are written for the Laplace transforms of the normal acceleration and pitch rate in terms of airplane system functions (i.e., the airplane responses to impulsive inputs), the transform of the gust, and the system functions of the control system. The system requirements to obtain perfect alleviation with one or both controls are determined, and the implementation of a system is found to be impractical. An analysis is made assuming perfect alleviation to be impossible and only one control to be available to obtain the desired alleviation. The equations of motion are written as convolution integrals involving the inverse transforms of the aircraft system functions and the gust input. Tobak seeks to minimize a linear combination of the normal acceleration and the pitch rate; namely, the mean-square error as defined by

$$\overline{\varepsilon^2} = \overline{q^2} + \frac{1}{a}\overline{(\dot{\alpha}')^2}$$

By proper substitution, $\overline{\varepsilon^2}$ is expressed as a sum of three integrals, involving one unknown function. Application of Weiner's optimum filter theory[28] results in a Weiner-Hopf integral equation which can be solved for the one unknown function. The formulation of the Laplace transform of the required control system is then obtained. Tobak applies the results of the analysis to a tailless, triangular-wing airplane flying at high subsonic speeds. The resulting control system is checked for adequate stability, significant alleviation, and practical feasibility. The control transfer function and the minimum mean-square error are obtained for various operating conditions and a turbulence scale of 300 feet. A range of the weighting factor "a" is found for which approximately 50% alleviation is obtained for both the normal acceleration and pitch rate. The control force required to obtain such alleviation is found to be about one-third of the gust force.

Experimental Studies

Considerable experimentation has been undertaken to investigate the problems associated with the determination and alleviation of the response of airplanes to atmospheric disturbances. Some of these experiments have attempted direct verification of the theoretical results of studies previously discussed[29, 30, 31], while others have been studies which could not be made theoretically[1, 19, 32]. Still others have been devoted to the measurement of the characteristics of atmospheric disturbances[12, 33], and the simulation of those disturbances in the laboratory[34, 35]. The experiments may be classified as laboratory (wind-tunnel) tests and field (free flight) tests.

Wind Tunnel Tests

Wind tunnel tests have been made to test various components and systems for gust alleviation, and to develop means of simulating atmospheric disturbances. Tests of alleviating systems and components generally have been made in gust tunnels where the models are subjected to step or ramp-type gusts. A majority of such experimentation has been conducted by, or with the support of, the NASA.

One early test program undertaken by NASA is reported by Donely and Shufflebarger[19]. The effectiveness of a long-period, dynamically overbalanced flap as a gust alleviation was tested. A rectangular wing, equipped with the overbalanced flaps, was subjected to sharp-edged and ramp-type gusts. The flap displacement was directly proportional to the upward displacement of the wing; hence, the system was not expected to be very effective for sharp-edged gusts. Theoretical analysis made of the same system was found to be in excellent agreement with the experiment. The flap is found to be effective for long gradient gust, but to have, also, an adverse effect on stability and control.

Tests were also made of the effectiveness of a torsionally flexible wing in reducing airplane accelerations due to gusts[1]. Models with rigid and torsionally flexible wings were flown through sharp-edged and ramp gusts and the pitch, normal acceleration, speed, and wing torsional deflection were measured. The alleviation obtained varied between 5% for the sharp-edged gust, and 17% for ramp gusts of 15-chord lengths. The torsional wing deflection increased the wing washout and, therefore, reduced wing bending moment. However, some type of leading edge control device was found to be required to eliminate flutter and control reversal. The use of wing torsion as an alleviation device appears to be impractical for this reason.

Mickleboro[32] made wind tunnel tests to evaluate a fixed spoiler, located near the wing leading edge, as a gust alleviator. A fixed spoiler, 2.5% of a chord length high and extending over 90% of the span, was located at the 10% chord point of the wing, and the model was flown through sharp-edged and ramp gusts. The spoiler was found to have no effect on the maximum acceleration due to sharp-edged gusts, but a 30% reduction was obtained for ramp gusts of 12-chord lengths. The practicability of the spoiler as an alleviator was undetermined because the results for negative disturbances were not obtained.

The effects of wing bending on the gust loads experienced by a sweptback wing were investigated by Reisert[2]. A model with the semi-chord line of the wing swept back at a 45 degree angle was prepared with the wings hinged along a line perpendicular to the semi-chord line. Flights were made with rigid wing and flexible wing models at 60 mph through sharp-edged gusts of the 10 ft./sec. velocity. The acceleration and pitching motions experienced by the models were compared. Responses of both models to ramp-type gusts were obtained theoretically by superimposing the sharp-edged gust responses. Reductions in normal acceleration of 8% for the sharp-edged gust and 14% for a ramp gust of 9-chord lengths were obtained. An adverse pitching motion was found to occur due to the wing bending and subsequent forward shift of the aerodynamic center. This pitching motion reduced the effectiveness of the flexible wing as an alleviator; hence, the use of such a system requires some means of reducing the adverse pitching motion.

Croom, Shufflebarger, and Huffman[16] tested combinations of fixed spoilers and deflectors as gust alleviators. Spoilers, deflectors, or both, were mounted on the wing of a transport model which was flown through sharp-edged gusts at 10 and 15 ft./sec. Spoilers were mounted on the upper surfaces and deflectors on the lower surface at the 12% chord position. Static aerodynamic tests revealed that a decrease in tail effectiveness and an increase in longitudinal stability were caused by both types of surfaces. The normal accelerations and pitch angles were recorded. The deflector reduced the maximum acceleration by 20% to 40% without a significant change

in pitching. The spoiler combinations were found to be effective also, but an appreciable increase in pitching resulted. The alleviation obtained was found to be relatively constant for gust gradients up to 20-chord lengths.

A series of wind tunnel tests which were designed to augment the power spectral density analyses was conducted by Lamson[31]. The aerodynamic admittance of a rigid wing in turbulent flow was calculated from the measured power density spectra of the lift and turbulence. The turbulence spectrum was measured by putting the output of a hot wire into a wave analyzer. The lift spectrum was calculated from the measured turbulence spectrum and the mechanical admittance of the wing. Hence, the aerodynamic admittance was obtained from

$$|\Phi(\omega)| = \frac{1}{|T(i\omega)|}\left[\frac{h(\omega)}{f(\omega)}\right]^{1/2}$$

where $\Phi(\omega)$ = complex aerodynamic admittance
$f(\omega)$ = turbulence power spectral density
$h(\omega)$ = displacement power spectral density
$T(i\omega)$ = mechanical admittance of the wing

The effects of span variations were determined by the use of sliding end plates. A 20% thick airfoil with a 2-1/2 inch chord was tested. The model was mounted on a floating plate balance with a Schaevitz pickup. The output of the pickup was fed to one of three instruments for the determination of the mechanical admittance. The instrument used depended upon the frequencies being measured. A wave analyzer was used for frequencies above 70 cycles per second, mechanical resonance of the balance system was used for frequencies between 10 and 70 cycles per second, and a Krohn-Hite low-pass filter was used for frequencies between 2 and 10 cycles per second. The mechanical admittance was obtained by measuring the displacement as a function of frequency for a constant amplitude magnetic force. The turbulence was created by the use of grids upstream of the model. The absolute value of the aerodynamic admittance was plotted as a function of the reduced frequency (k) for the airfoil, with and without end plates. With end plates and $k > 0.8$, the aerodynamic admittance obtained agreed with Sear's results. However, the results were less than those obtained by Sears for $k < 0.8$.

Attempts have been made to simulate atmospheric disturbances in wind-tunnels. One such attempt was made by Hakkinen and Richardson[34]. The series of tests constituted a two-phase program to (1) create sinusoidal gusts in a low-speed wind tunnel in order to obtain experimental proof of Sear's results, and (2) create a stationary, random disturbance in order to measure the velocity and lift power density spectra of a rigid airfoil as a check of the theoretically determined aerodynamic admittance. A constant

cross-section airfoil with a one-foot chord was mounted vertically spaning the height of a low-speed wind tunnel. A four-inch section in the center of the span was mounted in a floating manner supported by three load cells. Sinusoidal gusts were generated by a one-foot by five-foot wing oscillating in a vertical plane upstream of the test section. The rms gust velocity was found to be indistinguishable from free-stream turbulence. It was concluded that Sear's function can only be checked experimentally by use of a low-turbulence wind tunnel and with an oscillator capable of creating large downwash amplitudes.

Random disturbances were generated in the wind tunnel by use of a coarse grid located ten feet upstream of the test section. The scale of the turbulence generated by the six-inch mesh was found to be too small for close matching of the results. The magnitude of the rms fluctuations was found to be about 3% of the free-stream velocity. The turbulence measurements were made using hot-wire techniques, and the lift measurements were obtained from the load cells. These measurements were simultaneously recorded on magnetic tape which was played into a thermocouple squaring unit through a narrow-band filter to obtain the power spectral measurements. Because of difficulties encountered in calibration of the filter, accurate absolute measurements of the power spectra were not obtained. It was possible, however, to accomplish the main objective -- the determination of the transfer function between the input and output power spectra. This was obtained for frequencies between 3 and 150 cycles per second by running hot wire and load cell signals through the filter successively, thereby cancelling the unknown proportionality factors. Statistical errors were introduced by measuring power spectra as finite time averages, and the rms value of these errors was found to be approximately 5%. Theoretical analyses were made and the results were found to agree well with experiment at high reduced frequencies.

A facility for the automatic processing of randomly fluctuating data is discussed by Smith[36]. The random data are recorded on magnetic tape and played back into an analogue computer facility which performs the desired analysis and automatically plots the results. The facility consists of four basic units: (1) magnetic tape data storage and playback, (2) a probability distribution analyzer, (3) a power spectral density analyzer, and (4) a cross spectral density analyzer. The increase in reliability, due to the economy of obtaining the data from longer records, is found to more than compensate for the relatively small errors (approximately 10%) introduced by the use of analogue equipment.

Two methods of achieving the passage of a gust over a fixed model are discussed by Kuethe, Schetzer, and Garby[35]. A "Vortex Gust Generator" for introducing a disturbance in the flow upstream of a model

is built and tested in a small, open-return wind tunnel. The generator consisted of a venetian blind arrangement, mounted vertically upstream of the model. A spring-loaded mechanism allowed the angle of attack of the slats to be changed up to 10° and return to zero in 1/25 second. The vortex sheets shed by the slats were carried over the model to stimulate a gust. Tests of the pilot model were made at wind speeds of 15, 30, and 60 ft./sec., and the velocity measurements were made with hot-wire equipment. The model was a constrained two-dimensional wing for which the theory is well understood. A second method of simulating the passage of a gust over a model is by changing the boundary conditions at the tunnel wall such that an angle-of-attack change is caused to sweep past the model. A "Moving Bump Gust Generator" was designed and tested in the same wind tunnel to implement such a simulation. The wall boundary conditions are changed by moving an airfoil-shaped bump along the floor of the tunnel. The resulting flow field over the model simulates emergence of the model from a gust, the severity of which depends on the speed of the bump and the airspeed. The position of the bump is measured by a potentiometer, and may be measured within ± 0.05 inches. Hot-wire anemometers were used to measure the angle of flow to within ± 0.1 degrees. The normal force on the model was measured by a single-component balance system. The pilot tests were made in the small, low-speed tunnel, and a five-foot by seven-foot, low-speed tunnel was used to extend the results of the pilot tests to higher Reynolds numbers. The results of the tests on both types of gust generators demonstrated the feasibility of generating reproducible gusts of sufficient intensity and scale at Reynolds numbers high enough to permit extrapolation to full scale.

A system for the generation of a sinusoidally varying gust in a low-speed wind tunnel was designed and tested by Wade and Thom[37]. Two symmetrical airfoils were mounted vertically in the wind tunnel, on each side of the centerline, such that they could be rotated simultaneously about their respective quarter-chord lines. A constant speed motor was used to drive the vanes in an oscillatory manner at frequencies up to 50 cycles per second. Measurements of the flow velocity fluctuations were made with a directionally sensitive hot-wire probe. The phase lag and amplitude of the sinusoidal flow variation were measured at various stations along and across the wind tunnel test section. The wave developed in the test section was found to be a close approximation to a sine wave. The amplitude of the wave was found to be as much as 3 degrees for a specified frequency range.

Flight Tests

Test of full-scale airplanes in free-flight have been made to determine the effectiveness of alleviation devices and systems. Tests have also been made to obtain data for the determination of the characteristics of atmospheric turbulence. Kraft and Assadourian[38] made flight tests to

determine the effectiveness of a vane as a sensing device for an acceleration alleviation. The specific purpose was to determine whether or not a single vane, mounted ahead of the nose of an airplane, would give a sufficiently accurate measure of the average airplane angle of attack due to gusts over the entire wing span. A pair of mass-balanced, 4-inch by 5-inch balsa vanes were mounted on either side of a 5-foot boom in the nose of a C-47 airplane. The vane angle of attack was measured photographically inside the boom. Other measured quantities were normal acceleration, indicated airspeed, thrust axis inclination angle, and airplane angle of attack. The system was calibrated in steady level flight through smooth air at various indicated airspeeds. Flight tests through rough air were made at 150 mph, and the resulting vane angles followed closely the variation in normal acceleration. Hence, the vane was found to provide a good indication of the average angle of attack of the entire wing.

Kraft[39] reports the results of a flight investigation of a complete acceleration alleviation system. A twin-engine light plane was modified in accordance with the results of an analytical study[13] and flown through rough air. Full-span flaps were used, and auxiliary flaps were provided to obtain the proper downwash at the tail. The elevator was split into three parts; the two outboard parts being used to counteract the pitching moment due to flaps. The control column was geared to the flaps as well as the elevator, in order to accomplish changes in direction. The plane was flown through smooth and rough air at 150 mph and 2000 ft. altitude. The vane position, normal acceleration, and pitching velocity were recorded as functions of time. The power spectral densities of the recorded quantities were obtained by the use of analogue computer data reduction equipment[36]. The recorded time histories showed that the normal accelerations were reduced to about 1/2 to 1/3 those of the basic airplane. The pitching velocities were found to be about the same in both cases. Comparison of the power spectra of the basic and alleviated airplane indicated an alleviation of approximately 50% at the natural frequency of the airplane. The controllability of the alleviated airplane was tested by performing pull-up and hold maneuvers. The response to the pull-up was found to be slightly faster for the alleviated airplane.

A series of flight tests of the same airplane and control system, as discussed above, were performed by Cooney and Schott[30] to study the effect of the alleviation system on wing and tail loads. The strains at the wing root and 40% tail semi-span were measured to determine the strain distribution due to gusts.

The application of Generalized Harmonic Analysis to the rough air response problem requires a knowledge of the power spectral characteristics of the atmospheric disturbances. The first flight tests performed for the determination of such characteristics of rough air were conducted by Clementson[33]. He presented data and a method for obtaining the power spectrum of gust velocities in the short-period range of an airplane. The

results were applicable for gust wave lengths between 200 and 2000 feet. Chilton[12] performed flight tests to provide power spectral characteristics for turbulence wave lengths between 10 feet and 200 feet. Flow direction vanes were mounted on a fighter airplane to measure angle of attack and angle of sideslip. Tests were made with the airplane in a straight and level flight at 1000 feet in altitude in clear air. The measurements of Clementson[33] and Chilton[12] show that the power spectral density of atmospheric turbulence may be expressed as the following function of frequency:

$$\Phi(\Omega) = \sigma_u^2 \frac{L}{\pi} \frac{1+3\Omega^2L^2}{(1+\Omega^2L^2)^2}$$

This expression may be reduced to a simple proportionality which is valid for gust frequencies ordinarily of concern in gust analysis, as follows:

$$\Phi(\Omega) \propto \frac{1}{\Omega^2}$$

The results also indicate that at least two-dimensional isotropy exists in turbulent air.

A study which does not fit into the category of experimental flight tests, but which is pertinent to the discussion of the characteristics of atmospheric turbulence, is reported by Press, Meadows, and Hadlock[39]. A theoretical study was made in which the available measurements of the power spectra of atmospheric disturbances were reviewed, and estimates were made of the probability of encountering the various spectra in operation. The gust time histories were considered to be non-stationary (because of the dependence of turbulence intensity upon weather) Gaussian processes, varying only in rms gust velocity. Techniques were developed for the estimation of the probability distributions of rms acceleration and rms gust velocity from data available on peak accelerations due to rough air. The basic method assumed the turbulence to be locally Gaussian and stationary, and that the overall turbulence experienced consisted of a summation of exposures to elemental Gaussian processes for appropriate times. Rice's[40] relationship between the average number of maximums per second, exceeding a given value $[\overline{M(a_n)}]$ were applied to the elemental discrete conditions and summed over the various conditions. The resulting expression for $\overline{M(a_n)}$ was allowed to go to the limit to obtain a similar expression for gust velocities which cover a continuous range of values. The resultant expressions relate the mean-square acceleration $(\sigma_{a_n}^2)$ and $\overline{M(a_n)}$ for the cases in which rms gust velocity assumed both discrete values and a continuous range of values. The rms accelerations were estimated from operationally obtained $\overline{M(a_n)}$, and then transformed into the distributions of rms gust velocity by use of the airplane transfer function.

PROPOSED TECHNIQUE

The design of an automatic control system for the alleviation of aircraft response to rough air requires certain physical data. Some of the data may be obtained with sufficient accuracy by theoretical estimates, but most must be obtained by measurement. The data measurements that must be obtained are best seen by a short review of the theoretical aspects of the proposed approach to the design problem.

Theory

The primary objective is to design a control system that will alleviate the forces on the constrained airplane due to random gust disturbances. The components of the input which are most important from the standpoint of platform stability are those near the longitudinal short period of the airplane. Since this natural frequency is generally small[41], wake and apparent mass effects are assumed negligible.

The problem is formulated in terms of sixteen transfer functions, as shown in Figure 2. These transfer functions relate the forces and moments on the constrained airplane to the gust input, the control deflections to the gust input and airplane motion, the control forces to the control deflections, and the airplane motions to the forces due to the gust input and controls. The equations of motion may be written as follows:

$$(S_{11} + L_{11})w + (S_{12} + L_{12})\theta = Ge^{i\omega t}[T_1 + T_3 T_{13} + T_4 T_{15}]$$

$$(S_{21} + L_{21})w + (S_{22} + L_{22})\theta = Ge^{i\omega t}[T_2 + T_3 T_{14} + T_4 T_{16}]$$

where

$$L_{11} = T_{13}(T_5 + T_9) + T_{15}(T_6 + T_{10}) \qquad L_{21} = T_{14}(T_5 + T_9) + T_{16}(T_6 + T_{10})$$

$$L_{12} = T_{13}(T_7 + T_{11}) + T_{15}(T_8 + T_{12}) \qquad L_{22} = T_{14}(T_7 + T_{11}) + T_{16}(T_8 + T_{12})$$

The S_{ij} represent the differential coefficients in the airplane equations of motion with no alleviation system acting, and the L_{ij} represent the forces introduced if the gust sensor is influenced by the motion. The control system will effect the stability of the airplane if the L_{ij} are different from zero, but if $L_{ij} = 0$, the alleviator will act as an open-loop system. The L_{ij} will be zero if the following equalities are satisfied:

$$T_5 + T_9 = 0 \qquad T_7 + T_{11} = 0$$

$$T_6 + T_{10} = 0 \qquad T_8 + T_{12} = 0$$

A major design difficulty is to satisfy these equalities.

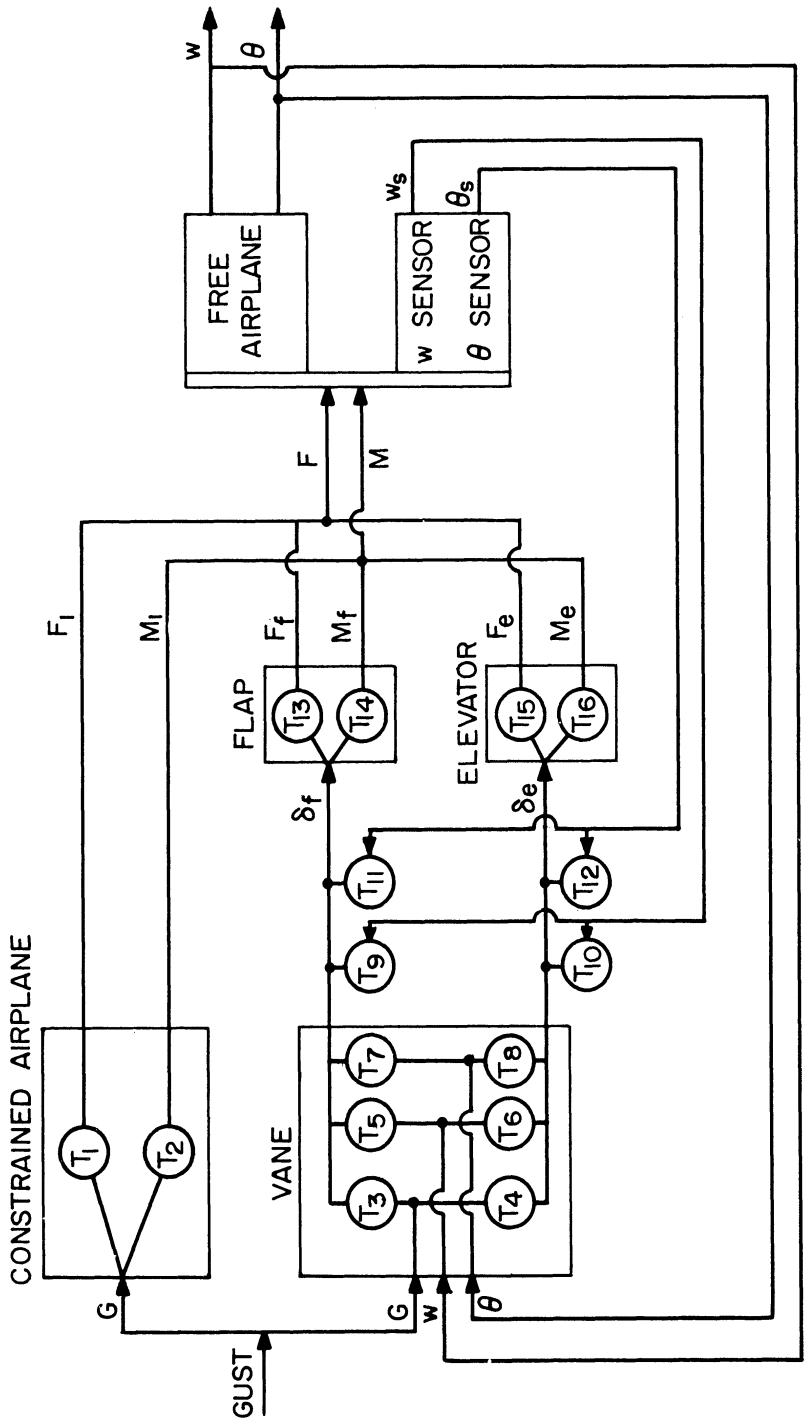

$$T_1 = \frac{F_I}{G} \qquad T_2 = \frac{M_I}{G} \qquad T_3 = \frac{\delta f}{G} \qquad T_4 = \frac{\delta e}{G}$$

$$T_5 = \frac{\delta f}{w} \qquad T_6 = \frac{\delta e}{w} \qquad T_7 = \frac{\delta f}{\theta} \qquad T_8 = \frac{\delta e}{\theta}$$

$$T_9 = \frac{\delta f}{w_s} \qquad T_{10} = \frac{\delta e}{w_s} \qquad T_{11} = \frac{\delta f}{\theta_s} \qquad T_{12} = \frac{\delta e}{\theta_s}$$

$$T_{13} = \frac{F_f}{\delta f} \qquad T_{14} = \frac{M_f}{\delta f} \qquad T_{15} = \frac{F_e}{\delta e} \qquad T_{16} = \frac{M_e}{\delta e}$$

Figure 2. Problem Formulation.

The velocities, w and w_s, shown in Figure 2, are the same quantities. They have been separated in the diagram because w is a geometric quantity that affects the vane directly, while w_s is a sensed quantity. Similar remarks apply to θ and θ_s. Hence, the dynamics of the sensors are neglected.

Experimental Procedure

The measurements necessary for the design and appraisal of the alleviator are to be obtained from wind-tunnel tests of a dynamically scaled model airplane. The test program[41] outlined below obtains sufficient measurements for the design and appraisal of the alleviation:

Test Program A

I. Stability Derivatives

A)	Static derivatives	-- C_{L_α}, C_{M_α}
B)	Damping derivatives	-- C_{M_q}, $C_{M_{\dot{\alpha}}}$
C)	Elevator power	-- $C_{L_{\delta_e}}$, $C_{M_{\delta_e}}$
D)	Flap power	-- $C_{L_{\delta_f}}$, $C_{M_{\delta_f}}$

II. Gust Input (Constrained Airplane)

Measure C_L and C_M for bump oscillating between 0 - 2 cps

III. Controls Input (Constrained Airplane)

Measure C_L and C_M for flap and elevator oscillating (separately) between 0 - 2 cps. Check against IC and ID for non-stationary effects.

IV. Short Period Check (Free Airplane)

Find short period by oscillating bump in neighborhood of 0.75 cps and noting resonance.

V. Time Lag of Alleviator (Constrained Airplane)

Measure phase shift between

1) bump position and flap displacement
2) bump position and elevator displacement

for a range of frequencies near <u>critical</u> (Critical frequencies will depend upon the period of the airplane and the frequency spectrum of the random atmospheric disturbances).

Test Program B

I. Input Cancellation (Constrained Airplane)

A) Find gearing for which gust input is cancelled by controls input at the critical frequency.

B) Check the effectiveness under "off critical" conditions. Select the best compromise.

II. Influence of Motion (Free Airplane)

A) Check the effectiveness (including stability) of the alleviator at and near critical frequency.

B) Eliminate effects of airplane motion on the gust sensor by detecting the motion with an accelerometer.

C) Check effectiveness and stability of the modified alleviator from 0 to 2 cps.

A dynamically scaled model airplane, a fixed mount and balance system, and a dynamic suspension system were designed and constructed for the tests outlined above. All items of Test Program A which did not require oscillation of the bump have been completed as a means of proof-testing the technique. The tests to date have been conducted in the low-speed, low-turbulence gust tunnel at the University of Michigan Aeronautical Engineering Laboratories. Wind tunnel tests to determine static characteristics of the model were performed with a constrained model, mounted on an internal strain-gauge balance system. Measurements of dynamic characteristics were made with the model mounted on a suspension system which had two degrees of freedom -- pitch and plunge. The gust input was simulated by the moving bump gust generator[35] previously discussed. A method of oscillating the bump has been developed and tested under no-flow conditions.

Model

A dynamically scaled model airplane was used for the experiments performed. The model was designed to be adapted to the type of gust generator used by placing the horizontal tail and elevator either in the conventional aft position or forward of the nose in a Canard configuration. The latter configuration was found to be the most suitable for use with the moving bump gust generator because a conventional configuration experienced a tail stall in the strong upwash near the bump leading edge. The model constructed was a 1/9 scale model of a prototype having the general size and shape of a straight-wing fighter airplane. The considerations of dynamic similarity and the details of the model, the supports and the controls, are discussed in subsequent paragraphs.

Dynamic Similarity

The airplane was considered to have degrees of freedom in plunging and pitching. The equations of motion were non-dimensionalized and the governing non-dimensional parameters were isolated in order to assure that the aerodynamic and inertia forces were in the same relation on the model as on the prototype. The wind tunnel axis system used in writing the equations of motion is shown in Figure 3. The origin of the axis system is located at the model support which is also the c.g. of the airplane. The equations of motion are written as follows:

$$\underline{\Sigma F_z = 0}$$

$$M\ddot{z} + \frac{\rho}{2} V_\infty^2 S m \frac{\dot{z}}{V_\infty} - \frac{\rho}{2} V_\infty^2 S_t m_t \frac{l\dot{\theta}}{V_\infty} + \frac{\rho}{2} V_\infty^2 S m \theta = 0$$

$$\underline{\Sigma M = 0}$$

$$I_{yy}\ddot{\theta} - \frac{\rho}{2} V_\infty^2 S c \frac{c}{2V_\infty} C_{M_q} \dot{\theta} - \frac{\rho}{2} V_\infty^2 S c\, C_{M_\alpha} \theta - \frac{\rho}{2} V_\infty^2 S c\, C_{M_{\dot{\alpha}}} \frac{\dot{z}}{V_\infty} = 0$$

Define the following non-dimensional parameters:

$$\dot{z}' = \frac{\dot{z}}{V_\infty} \qquad k_y' = \frac{k_y}{c} \qquad D' = \frac{D}{V_\infty/c}$$

$$\mu = \frac{2M}{\rho S c} \qquad t' = \frac{t V_\infty}{c}$$

The two non-dimensional equations of equilibrium become:

$$(\mu D' + m)\dot{z}' + \left(-m_t \frac{S_t}{S} \frac{l_t}{c} D' + m\right)\theta = 0$$

$$(C_{M_{\dot{\alpha}}})\dot{z}' + \left(-\mu k_y'^2 D'^2 + \frac{C_{M_q}}{2} D' + C_{M_\alpha}\right)\theta = 0$$

The dynamic response of the model and prototype will be similar if the following coefficients are identical:

$$\mu,\ k_y,\ m,\ m_t,\ \frac{S_t}{S},\ \frac{l_t}{c},\ C_{M_\alpha},\ C_{M_q}$$

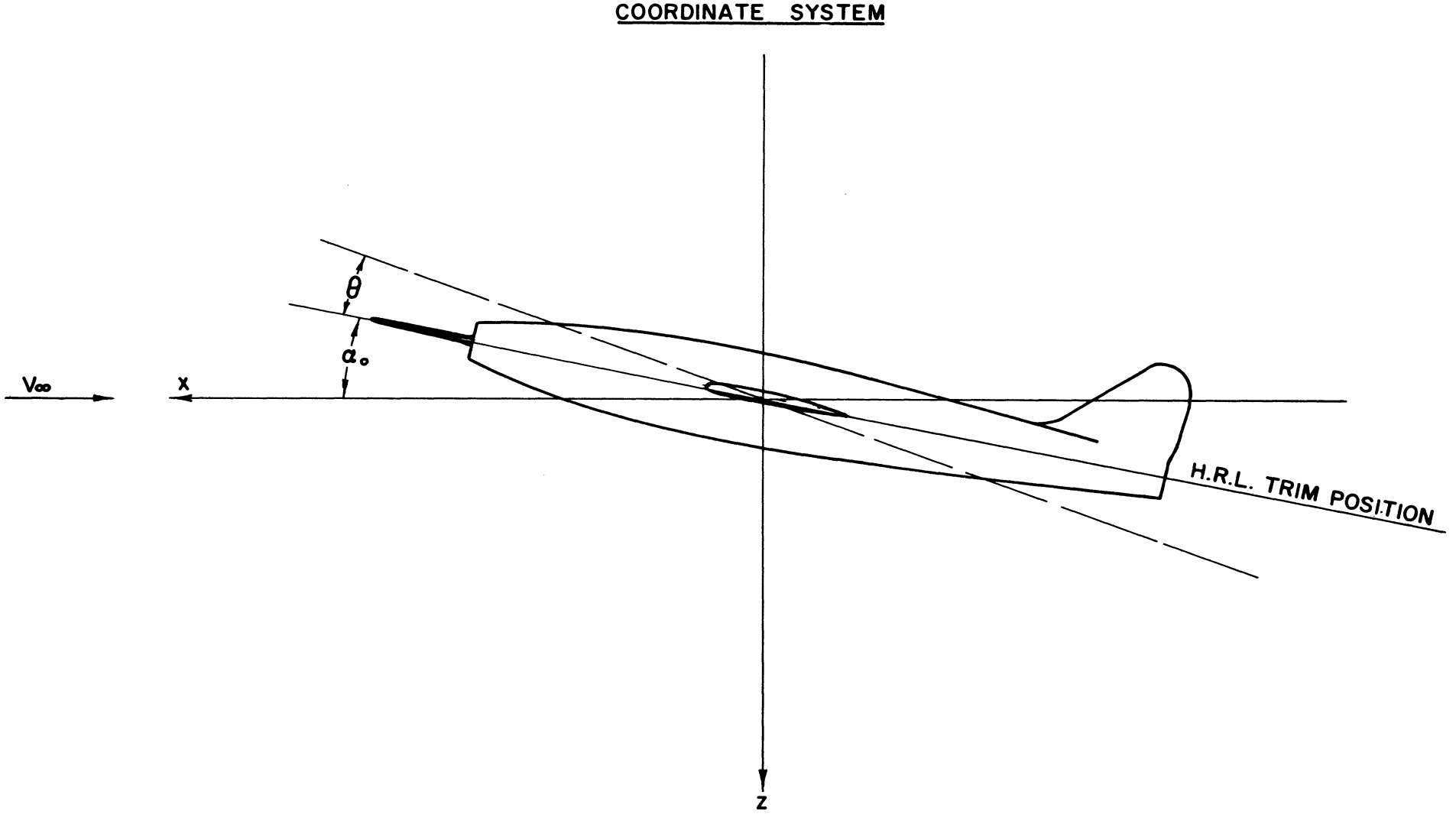

Figure 3. Coordinate System.

Hence, requirements are placed on the mass, mass distribution, and aerodynamic coefficients. The aerodynamic requirement implies that the Reynolds number and Mach number for the model and prototype are equal and that the model and prototype are geometrically similar. Aerodynamic interference effects that have been omitted from the equations are strongly influenced by the trim angle of attack (α_o); therefore, the further requirement is imposed that α_o must be equal for the model and prototype.

A scale factor β is defined as follows:

$$\beta = \frac{\text{size of model}}{\text{size of prototype}}$$

Hence, for the model and prototype to have the same value of μ, k_y, and α_o, the following equalities must be satisfied:

$$\frac{M_m}{M_p} = \beta^3 \qquad \frac{(V_\infty)_m}{(V_\infty)_p} = \beta^{1/2}$$

$$\frac{(W/S)_m}{(W/S)_p} = \beta \qquad \frac{(k_y)_m}{(k_y)_p} = \beta$$

Consequently, it is not possible to duplicate Reynolds numbers and Mach numbers simultaneously.

A comparison of the weight, wing-loading, and flight speed of the 1/9th scale model with those of its prototype is shown in Table I.

Table I

	Model	Prototype
W (#)	20	14,600
W/S (#/ft²)	5.95	60
V_∞ (ft/sec)	100	300

The trim lift coefficient for the model is

$$C_L(\alpha_o) = \frac{W/S}{q} = \frac{5.95}{11.9} = 0.50$$

Construction Details

The model used in the experimental portion of the program was not intended to be a replica of any particular aircraft now in existence. Instead, its design was dictated by the objective of the study and the capa-

bilities of the test facilities. Since the objective of the problem was to determine the control laws which must be followed to alleviate the response of a rigid aircraft to symmetrical disturbances, the model was constructed without regard to simulating aeroelastic effects. Also, since the disturbances are to be symmetrical (i.e., with respect to the plane of symmetry of the model), the model was constructed without such lateral control devices as dihedral and movable rudder.

The model was designed to simulate as closely as possible, within the restrictions of the test objectives and facilities, some realistic but hypothetical, aircraft. The size of the model, which was dictated by the size of the wind tunnel to be used, indicated that the model would be about a 1/9 scale model of a typical modern fighter aircraft. Hence, the physical characteristics were derived by applying the dynamic similarity conditions to the corresponding characteristics of an aircraft with a wing loading of 60 #/ft.^{2}. The characteristics thus obtained are presented in Table II.

The actual configuration of the model, as shown in Figures 4 and 5, is a low-wing monoplane with the horizontal tail mounted slightly forward of the nose. The tail was mounted in this position to prevent a tail stall when generating the gust with the moving bump. The unswept wing and elliptical fuselage cross-section were chosen to render the model construction as simple as possible. The wing contour at all stations is that of a standard NACA 2415 airfoil, and the tail contour is that of a symmetrical NACA 0009 airfoil.

The model has full-span wing flaps which may be displaced more than $\pm 45°$. The tail has full-span elevators which also may be displaced more than $\pm 45°$. Provisions have also been made to mount the horizontal tail in the conventional aft position, as shown in Figure 6.

The range of C.G. positions of the model, with respect to the wing aerodynamic center, are shown in Figure 7.

Instrumentation

Dynamic Suspension System

In certain of the tests, the model is suspended by a system which allows it to pitch and plunge in response to the generated disturbance. This suspension system is shown in Figures 8, 9, and 10.

The internal tube (a) supports the model on the yoke (b) and is free to translate vertically through the external tube (e). The ball bushings (c) reduce the friction to a negligible amount. The external tube (e) is fixed to the collar (f) which is rigidly attached to the floor of the tunnel. The model is mounted on the yoke at its center of gravity with a 1/4 inch diameter steel rod as shown. The ball bearings which are located in the yoke reduce

Table II

Model Characteristics

Weight (W)	20.0 lbs.
Radius of gyration (k_y)	8.3 in.
Wing --	
area (S)	485 in.^{2}
Span (b)	47.4 in.
taper ratio (λ)	0.52
aspect ratio (AR)	4.6
root chord (c_r)	13.6 in.
tip chord (c_t)	7.0 in.
mean chord (c_m)	10.6 in.
section (all stations)	NACA 2415
Tail --	
area (S_t)	40 in.^{2}
span (b_t)	10 in.
taper ratio (λ_t)	0.67
aspect ratio (AR_t)	2.5
mean chord (c_{m_t})	4.0 in.
Length (l_t) - tail aft	24.73 in. aft
" - " forward	23.98 in. fwd
section (all stations)	NACA 0009
Flap area (S_f)	111 in.^{2}
Elevator area (S_e)	40 in.^{2}

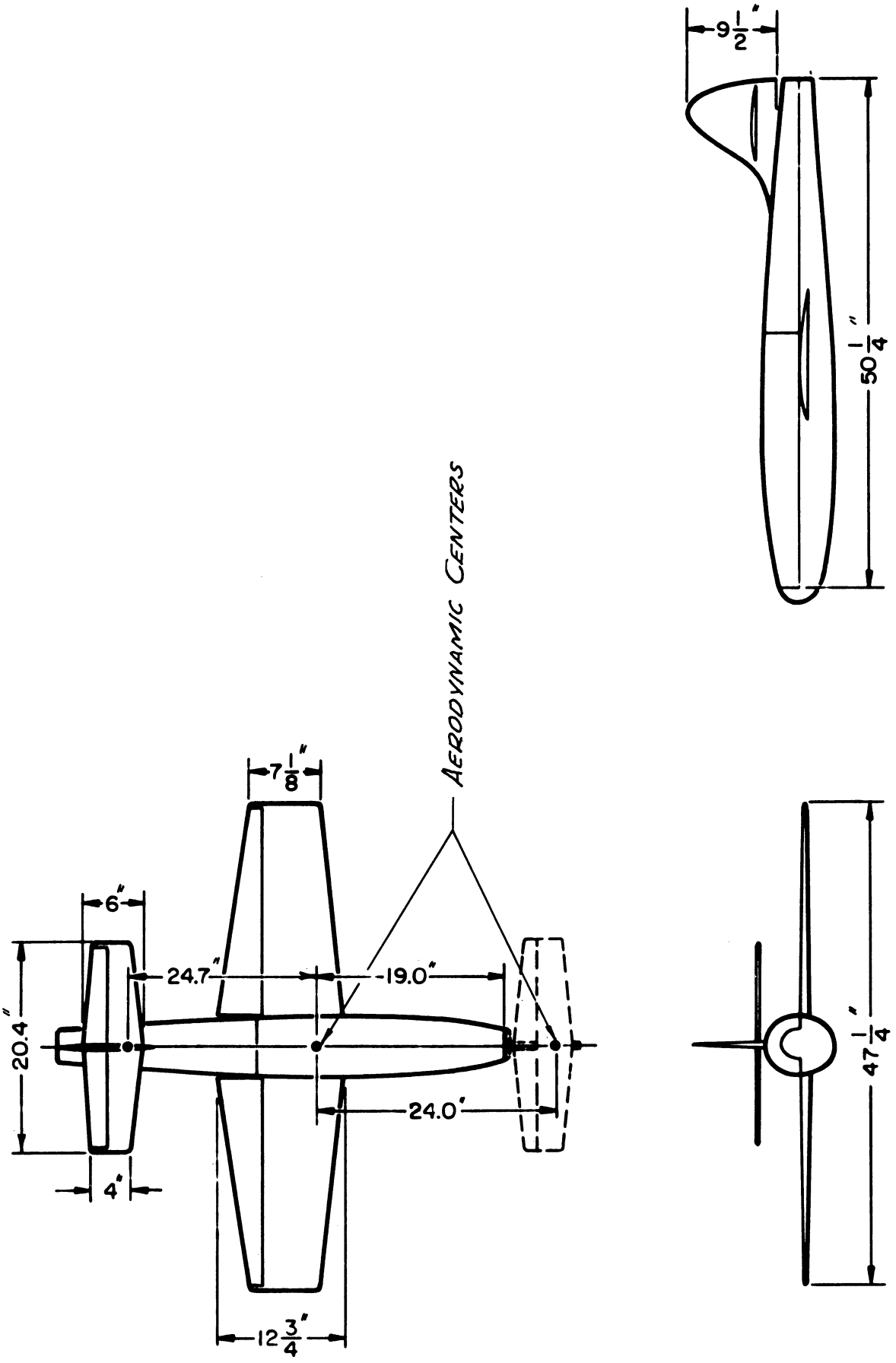

Figure 4. Model Configuration.

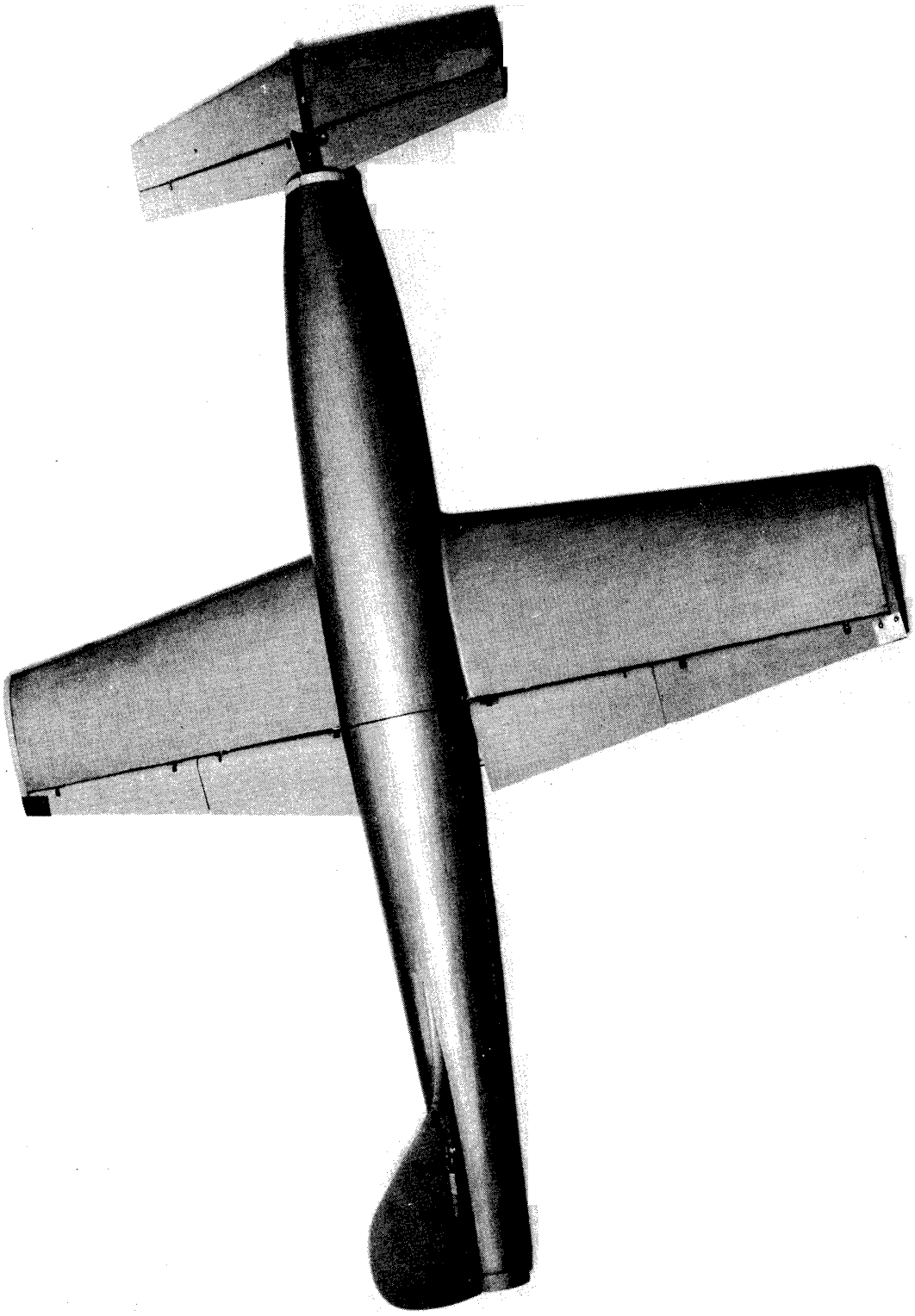

Figure 5. Model - Canard Configuration.

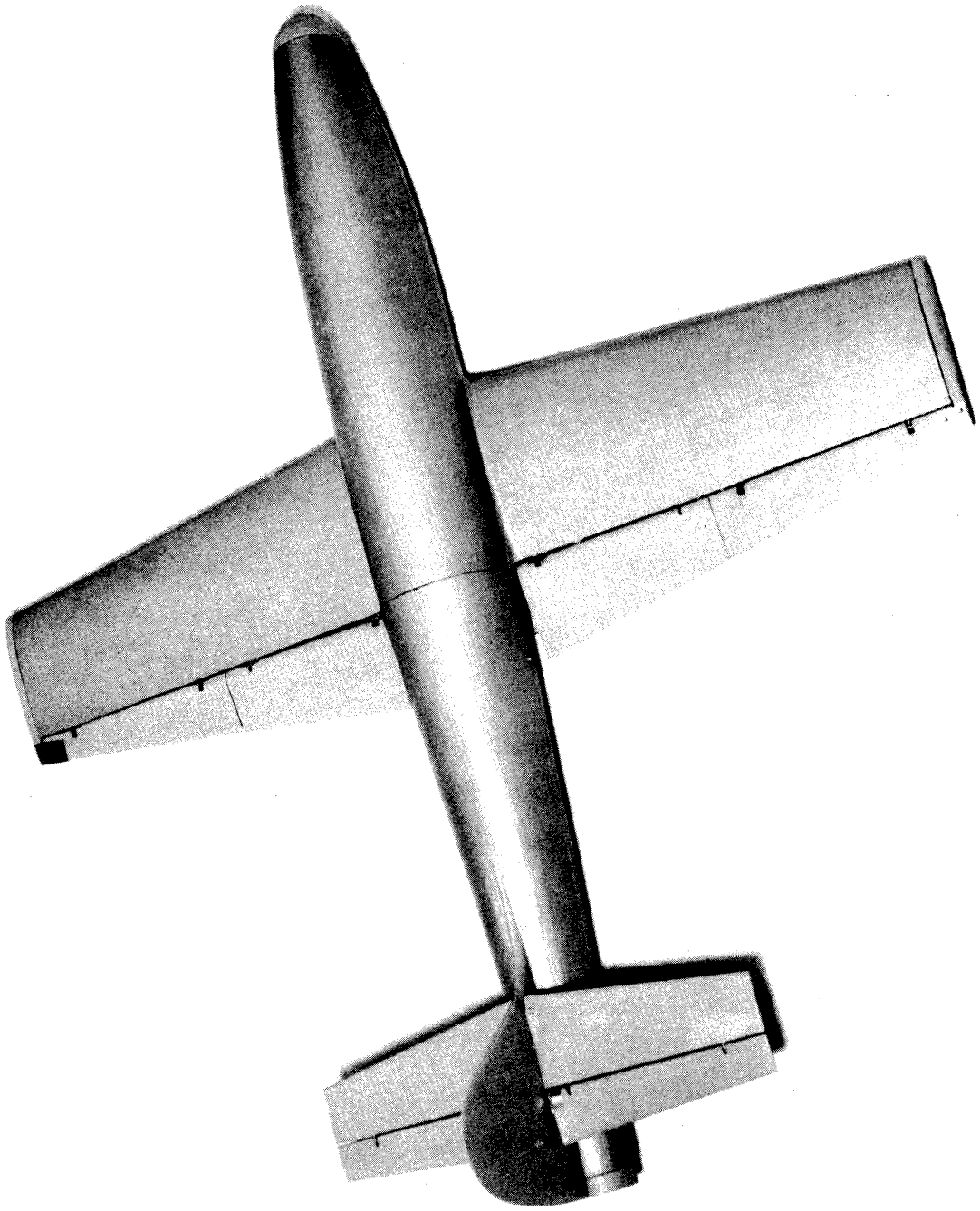

Figure 6. Model - Conventional Configuration.

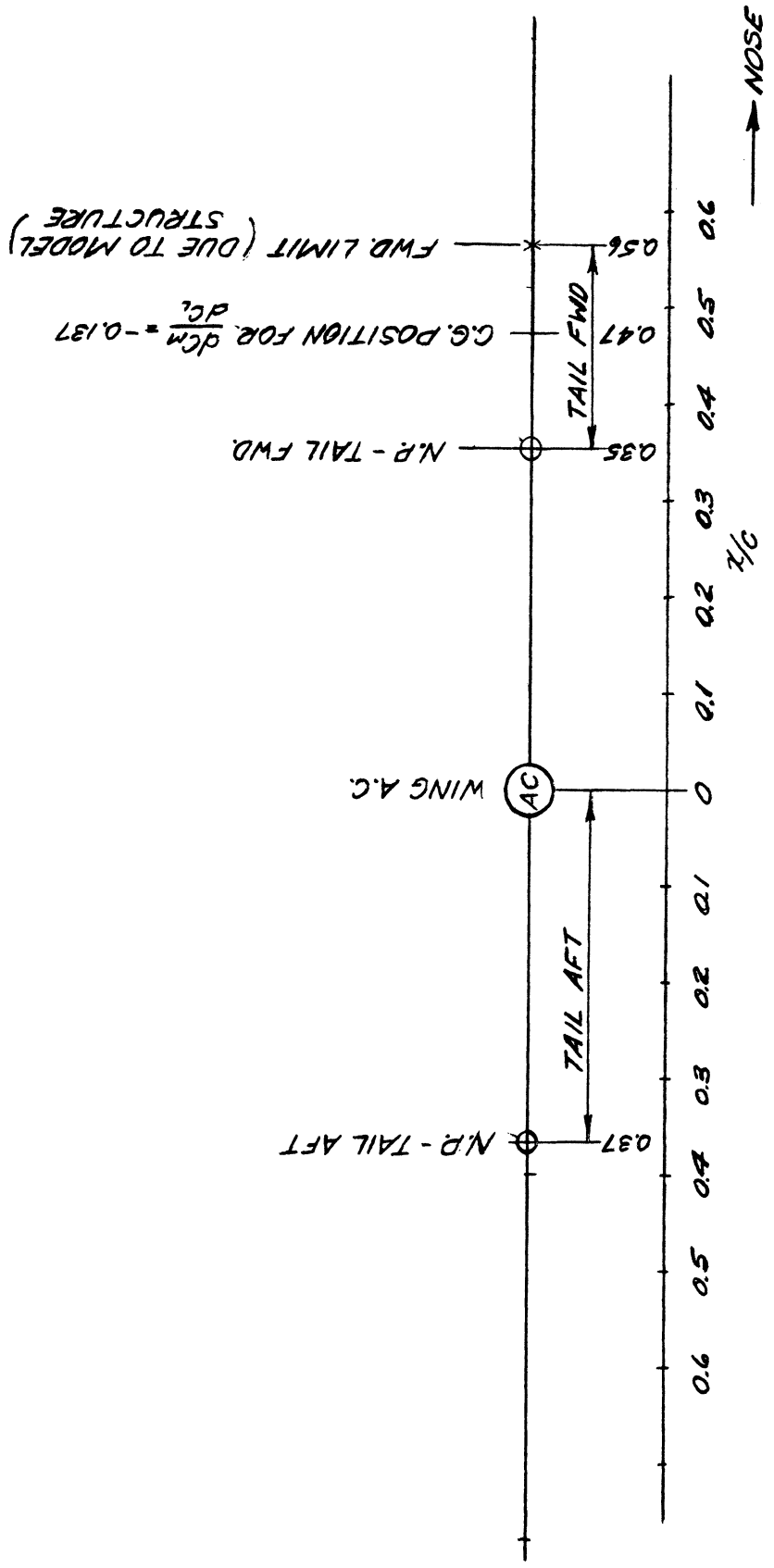

Figure 7. Limits of c.g. Travel in Relation to Wing Aerodynamic Center.

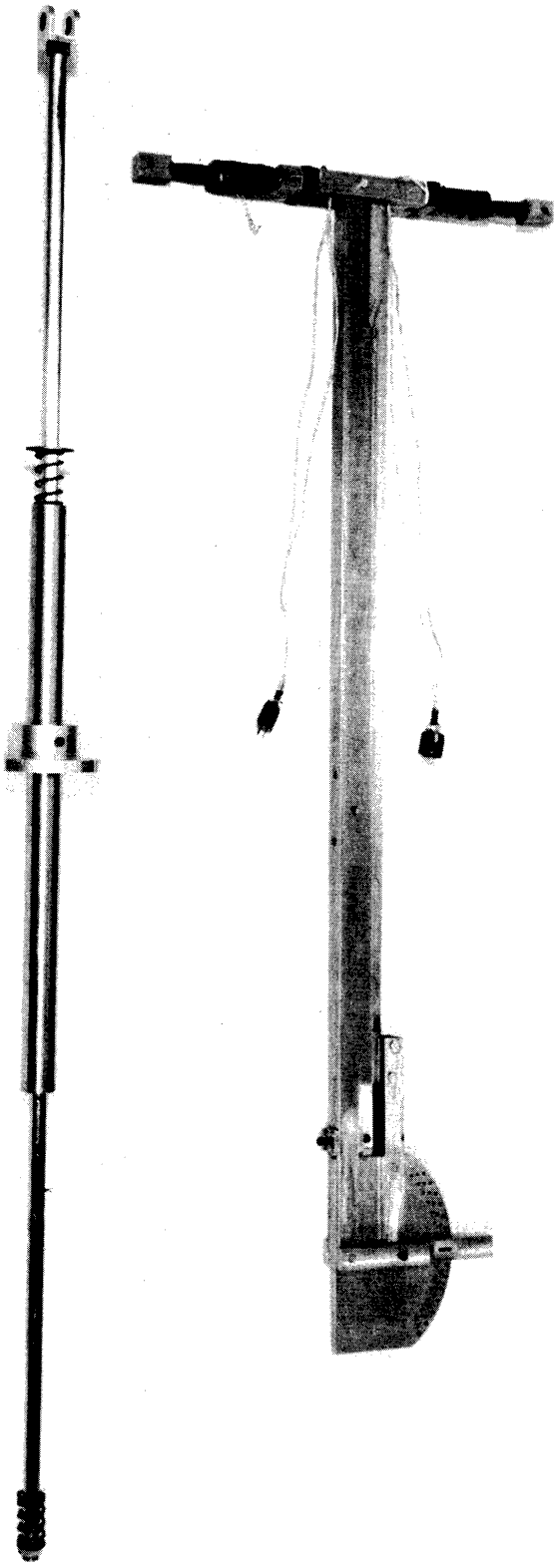

Figure 8. Model Suspension Systems.

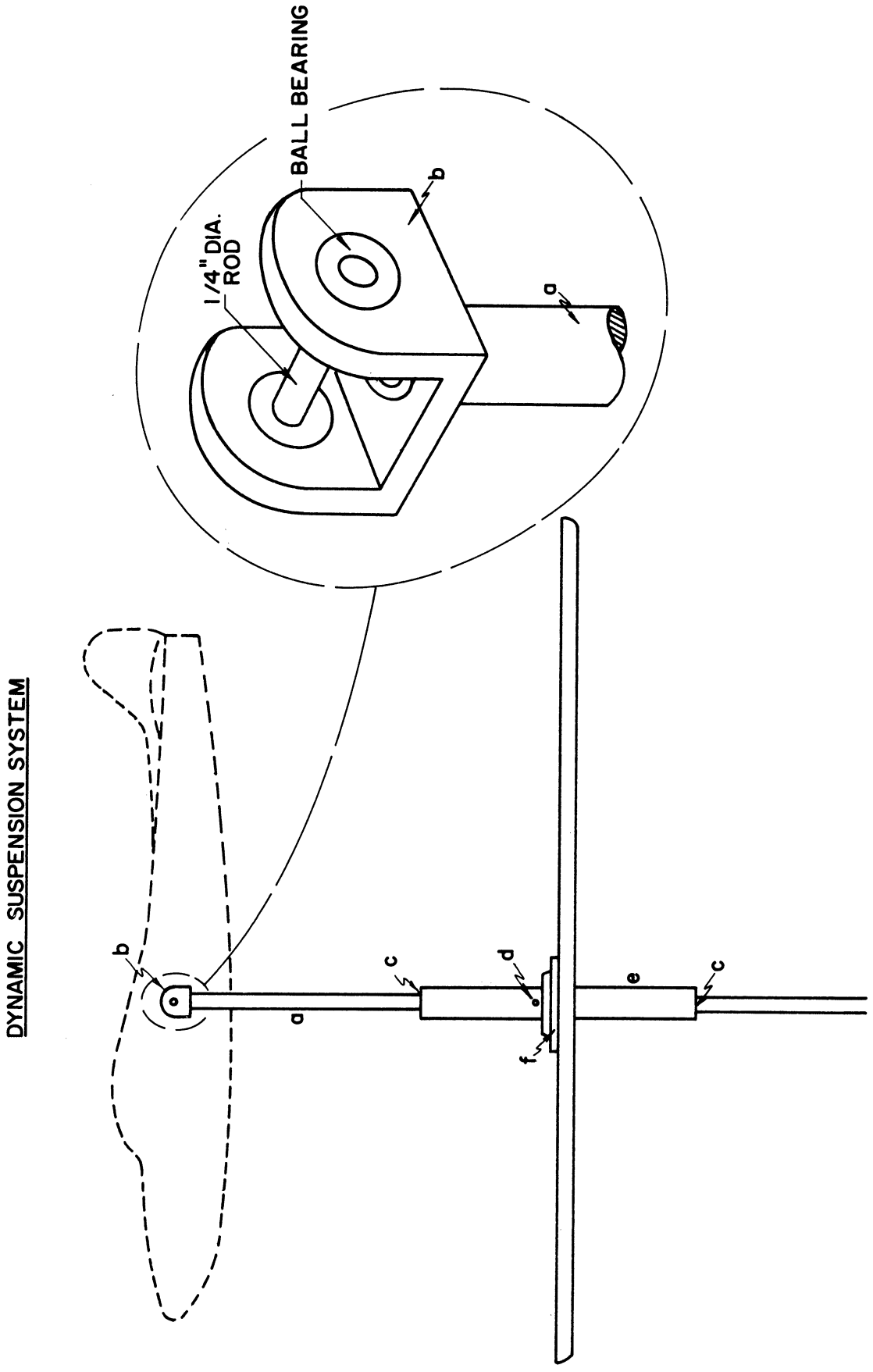

Figure 9. Dynamic Suspension System.

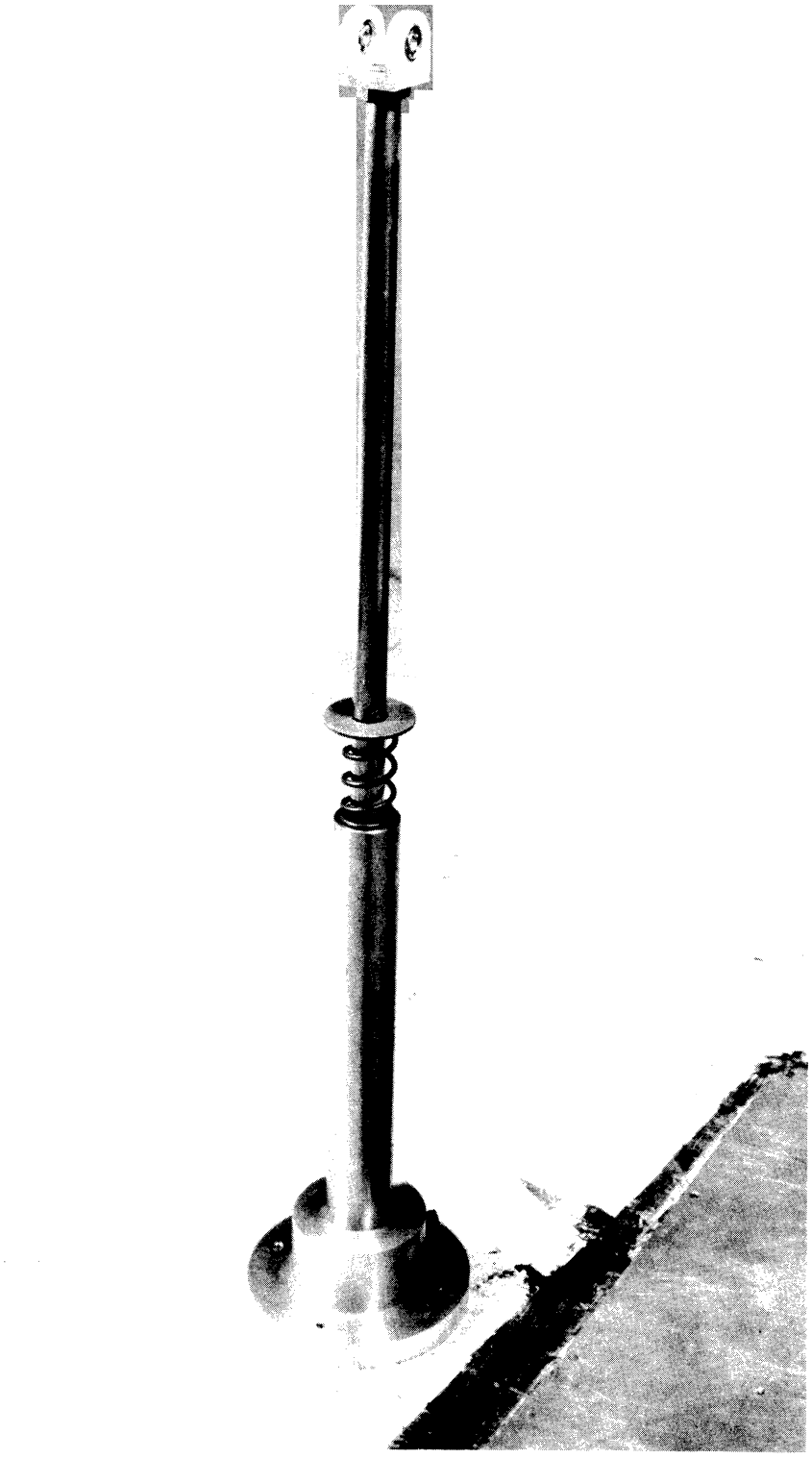

Figure 10. Dynamic Suspension System Installed in Wind Tunnel.

the friction in this connection to a negligible quantity.

This suspension system allows the model to perform vertical translation of its c.g. and pitching motion about its c.g.

Pilot tests on this suspension system have been made to determine if the model could be stabilized in the wind tunnel, and if a reasonable response to a disturbance could be obtained. Positive answers to both of these questions were found.

Fixed Mount and Balance System

The mount to be used to support the constrained model is shown in Figure 8, 11, and 12. It consists of a steel post and rail about four feet long, mounted in a parallelogram arrangement. The post is fixed to the floor of the tunnel and the rail is free to slide in a groove in the post. The position of the rail is determined by the position of the handle at the lower end of the post. The handle is pinned to both the post and the rail and is held in position by a pin through the handle and one of the holes through the sector. The purpose of this arrangement is to make it possible to change the angle of attack of the model without entering the tunnel test section. The sector allows the control of the angle of attack to 2° intervals. Set screws are provided at the lower end of the post to allow a much finer adjustment of the angle of attack.

The model is attached to the fixed mount through the balance system, as shown in Figure 13. This balance system is essentially a beam pinned to the model at each end and to the mount at two points near the center. Four Huggenberger strain gages are bonded to the beam at each of the notches to form two Wheatstone bridges. A load applied to the model causes an unbalance of the bridges, and thereby generates an output signal from each bridge. These output signals are recorded on two channels of a Sanborn recorder.

Control System

Servosystems were designed and fabricated to operate the flaps and elevators in such a manner as to cancel, as nearly as possible, the forces and moments applied to the model by the generated gust. Small electric motors drive the flaps and elevators through gear trains, and rotary potentiometers providing position feedback. The motors were driven by signals provided by a portable analogue computer. A block diagram of the flap control system is shown in Figure 14. The elevator control block diagram is similar to that of the flap control. Figures 15 and 16 are sketches of the control hardware assemblies.

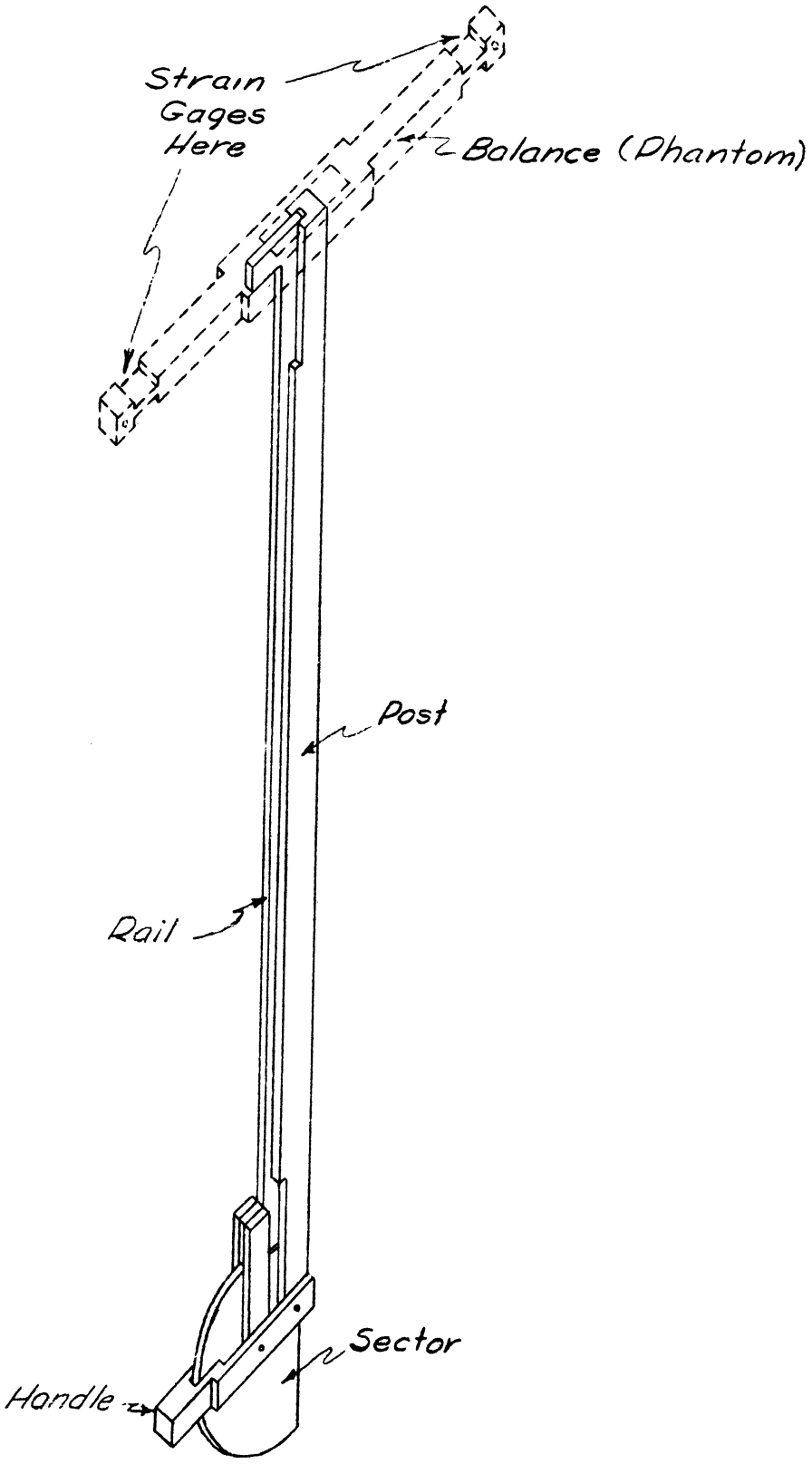

Figure 11. Fixed Mount and Balance.

Figure 12. Fixed Mount Installed in Wind Tunnel.

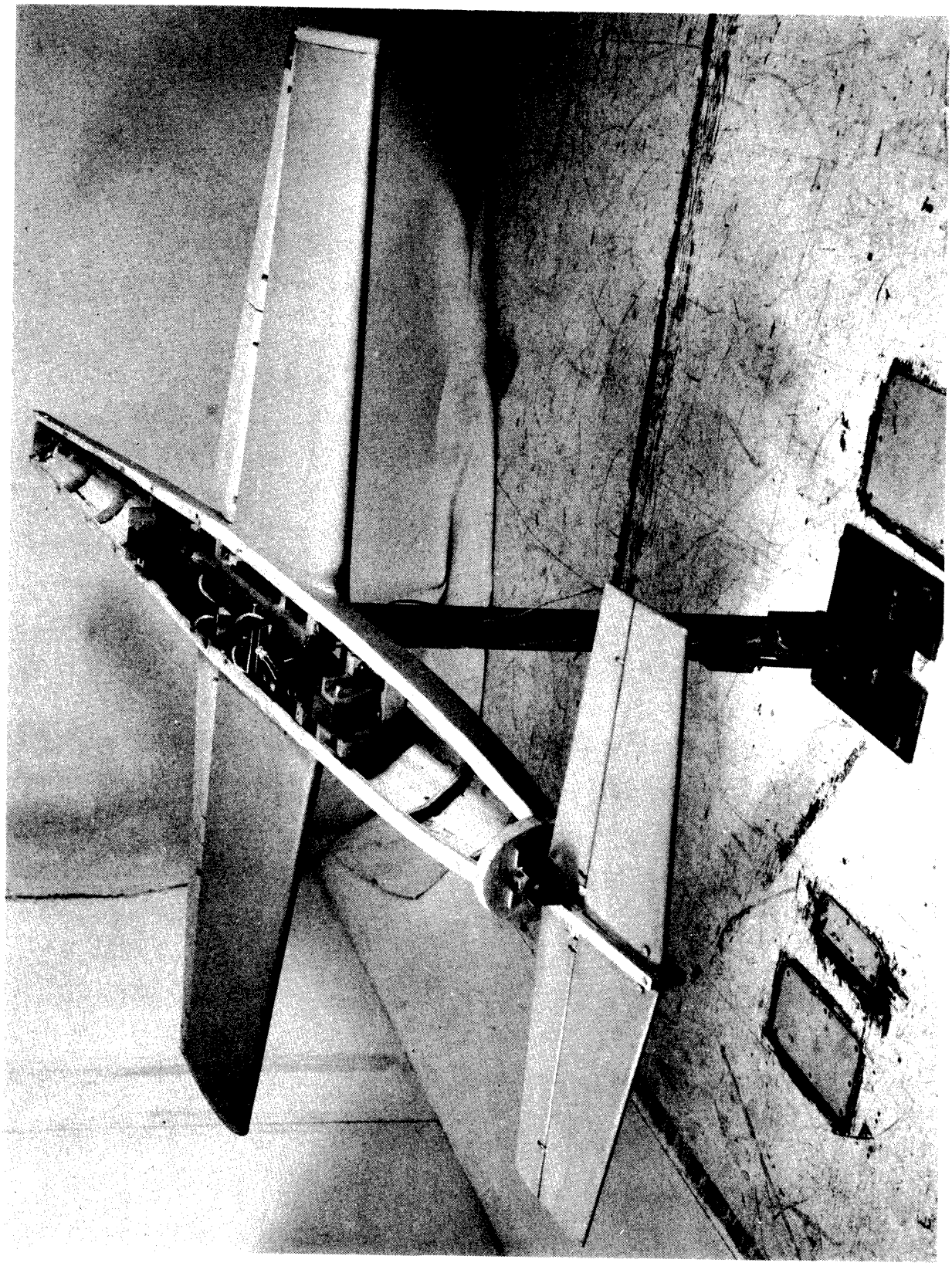

Figure 13. Model Mounted on Balance System.

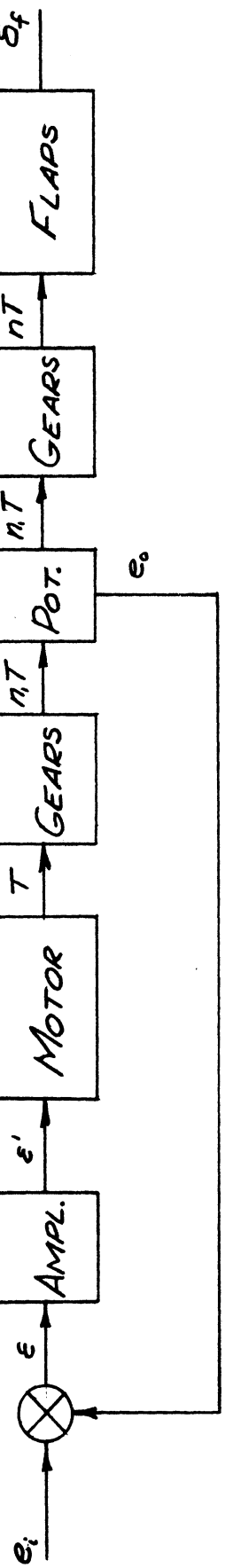

Figure 14. Block Diagram of Flap Controls.

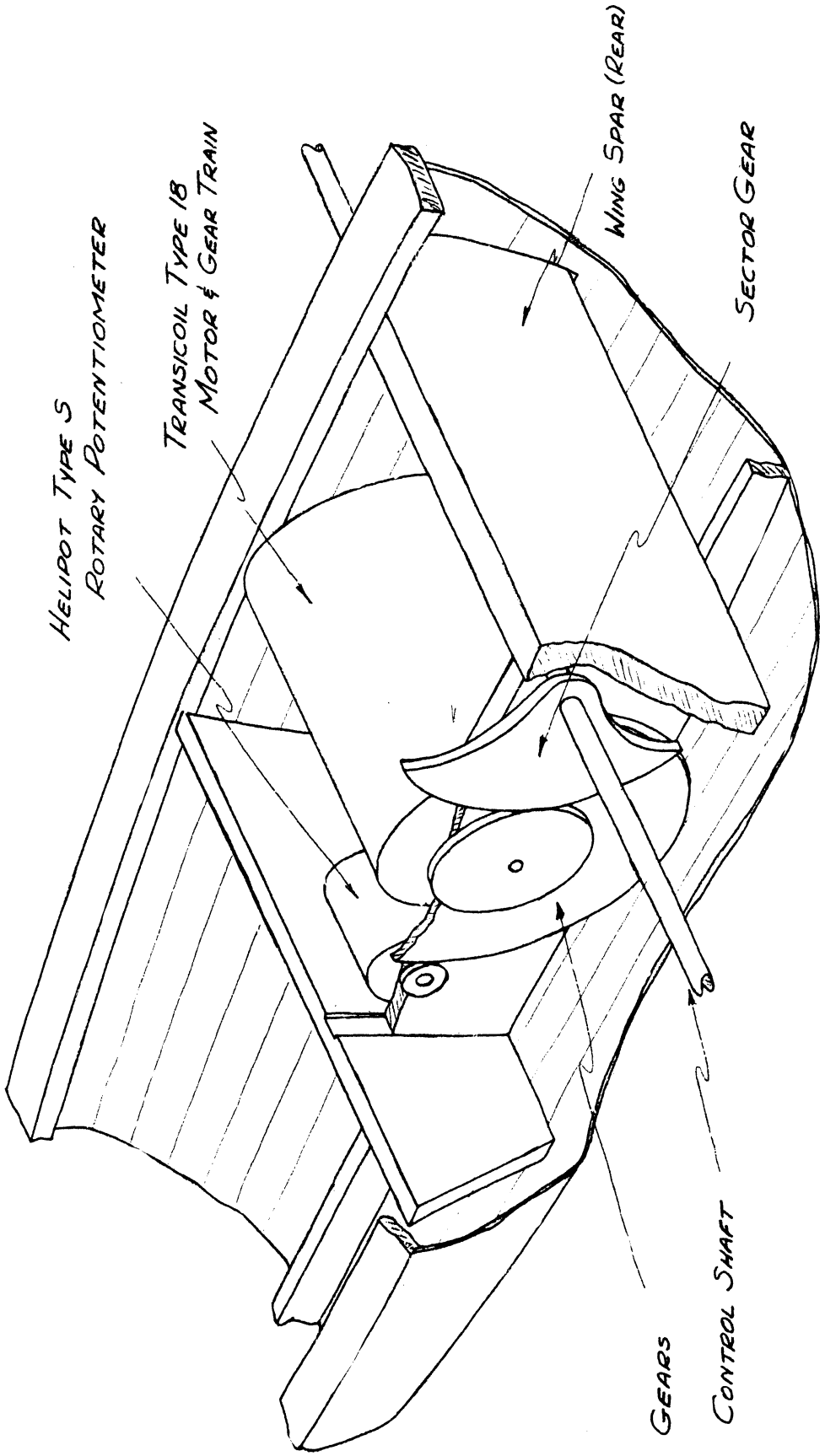

Figure 15. Flap Control Servomechanism.

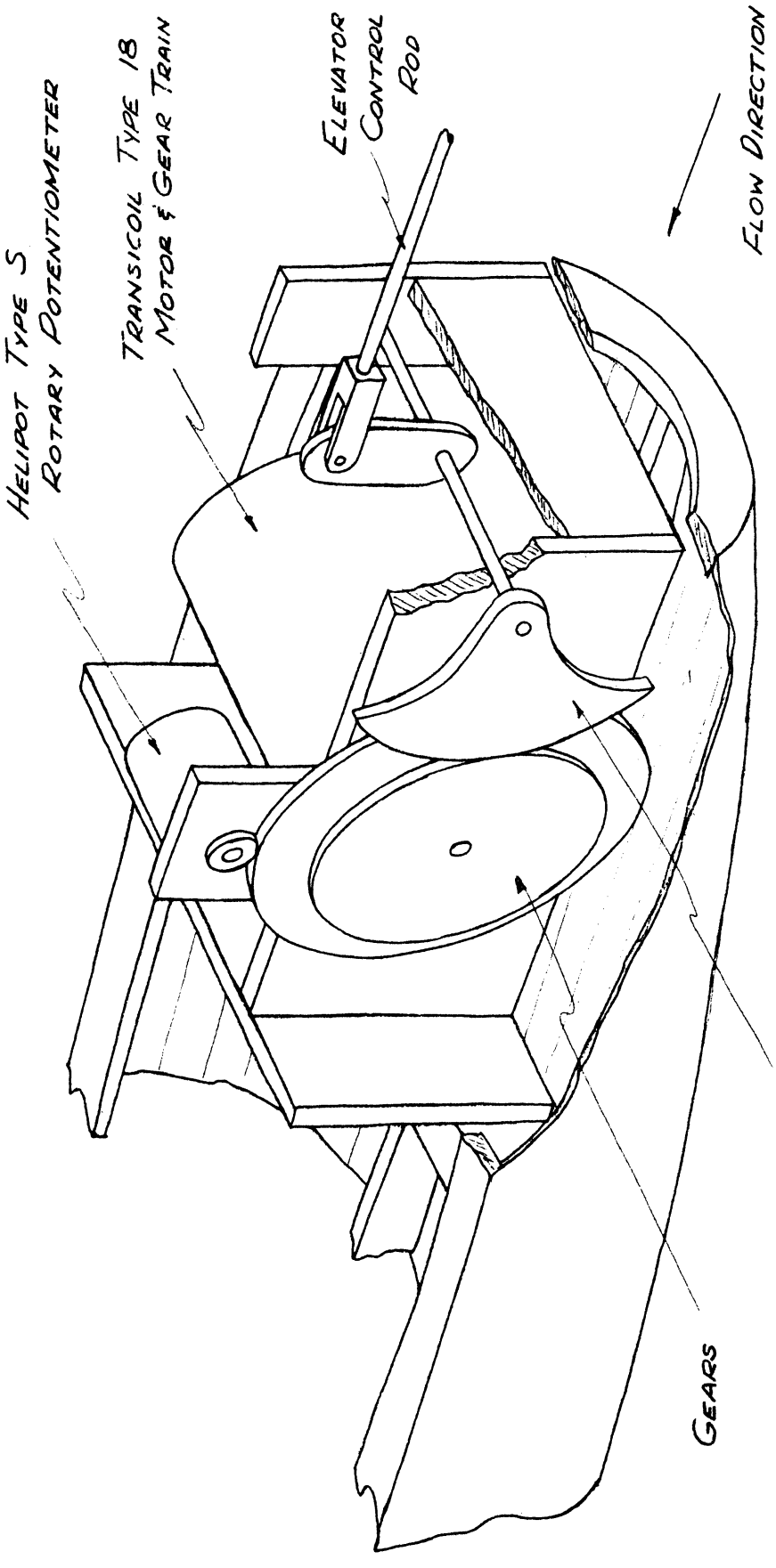

Figure 16. Elevator Control Servomechanism.

Disturbance Sensor

Some type of device is required which senses the presence of the disturbance. At present, it is planned to employ a constrained-vane type of sensor. A vane of small mass is mounted on the model, and electrical strain gauges are bonded to the vane so as to detect the force on the vane. The generated disturbance changes the angle of attack and thereby exerts a force on the vane which is detected by the strain gauges. The output signal thus generated is used as inputs to the flap and elevator control systems.

Pitch and Plunge Sensors

As outlined in the second part of the problem, the motion of the model is removed from the output of the vane by adding signals from pitch and plunge sensors directly to the elevator and flap. Instruments are required to sense both the velocity w and the pitch angle θ. The use of accelerometers to measure the pitch and plunge accelerations is suggested. The outputs of these instruments may be integrated with operational amplifiers to obtain w and θ.

Disturbance Generator

The disturbances are generated in the windstream by using the Moving Bump Gust Generator [35]. A sketch of the gust generator is shown in Figure 17. The bump is oscillated fore and aft by use of the mechanism indicated in the sketch. A "T" bracket is attached to the lower side of the bump and extends through the floor of the wind tunnel test section. Two sets of extension coil springs are attached to the bracket, parallel to the flow direction, and thus provided a lightly damped mass-spring system which tended to oscillate at a natural frequency defined by the mass of the bump and the spring rates. A forcing function was applied to the bump by a variable speed motor through the pulley-crank-spring arrangement shown. The anchor of the upstream spring is adjustable to provide a spring force which counteracts the unperturbed aerodynamic drag on the bump and allows the undisturbed bump to be in the center of its travel with the wind tunnel in operation. Resulting bump motion is a nearly sinusoidal oscillation with peak-to-peak amplitude of ten inches. The frequency of oscillation is varied by changing the extension coil springs. A time trace of the bump position obtained at zero wind velocity and a

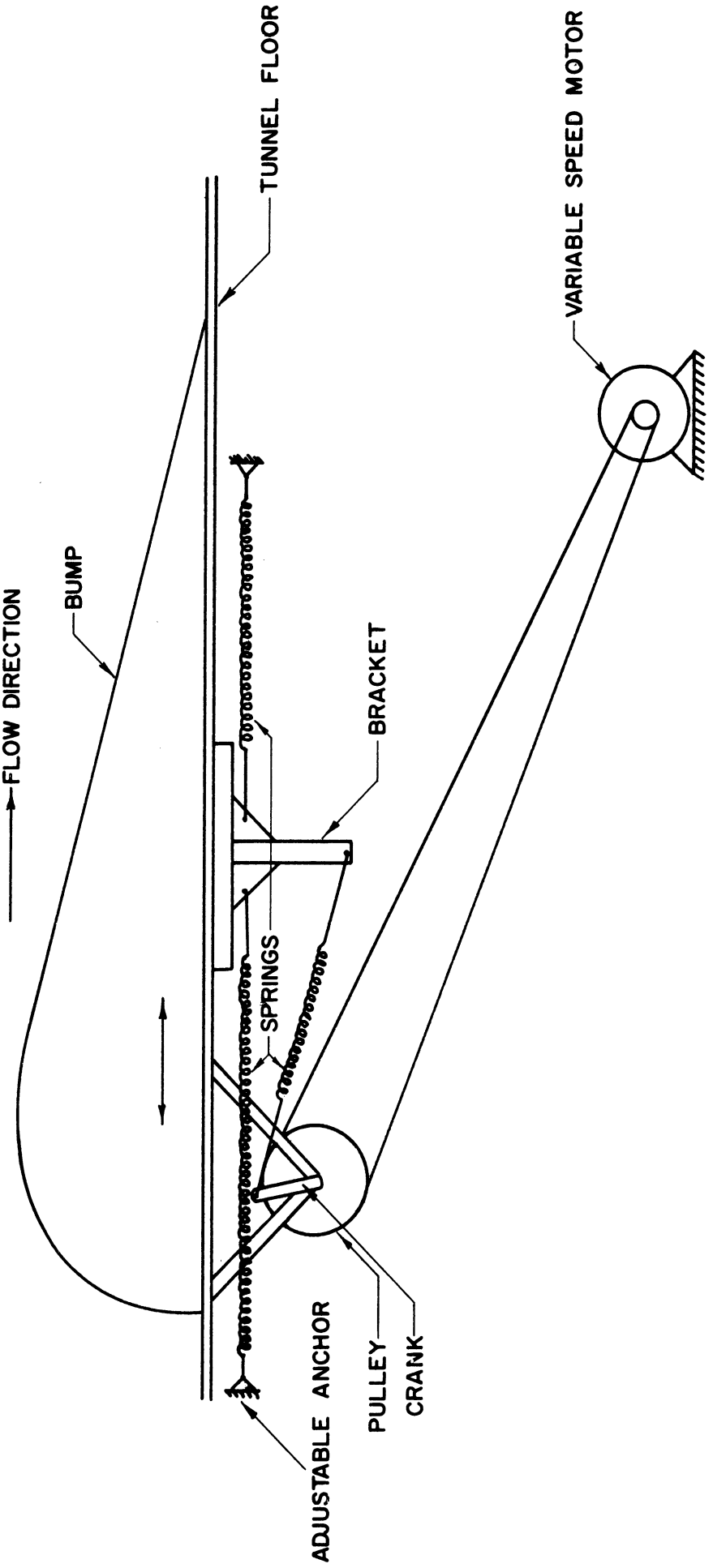

Figure 17. Disturbance Generator.

specific set of springs is shown in Figure 18. The oscillation shown has a frequency of about one cycle per second.

Results

A dynamically scaled wind tunnel model has been designed and constructed. The model has movable flaps and elevators which are controlled by servosystems and driven in response to signals from an analog computer. An internally mounted two-component balance system has been constructed, using bonded Huggenberger electrical strain gages. The balance system calibration curves are shown in Figure 19. The stability derivatives and controls input (Parts I and III - Test Program A) have been measured and are discussed below.

A means of obtaining sustained oscillations of the gust generating bump has been devised and tested under no-flow conditions. The bump was found to oscillate in a near-sinusoidal manner. A dynamic model suspension system which allows the model freedom to pitch and plunge has been designed, constructed, and subjected to pilot tests. The pilot tests indicate some stiction due to the deflection of the movable rod.

The curves from which the static-stability derivatives were measured are shown in Figures 20 and 21. Curves defining the elevator and flap power are presented in Figures 22 through 25. The following numerical values were obtained for these derivatives:

$$C_{L_\alpha} = 0.070 \ deg^{-1} \qquad C_{M_{\delta_f}} = -0.011 \ deg^{-1}$$

$$(C_{M_\alpha})_{\substack{\alpha=6^\circ \\ \delta_f=0}} = -0.0076 \ deg^{-1} \qquad C_{N_{\delta_e}} = 0.0022 \ deg^{-1}$$

$$C_{N_{\delta_f}} = 0.022 \ deg^{-1} \qquad (C_{M_{\delta_e}})_{\alpha=0} = 0.0043 \ deg^{-1}$$

The derivative C_{M_α} was found to vary significantly with α and δ_f ; hence, the value shown was taken for an unperturbed angle of attack of 6° and a flap deflection of zero. Similarly for $C_{M_{\delta_e}}$. The following value was obtained for the damping derivative:

$$C_{M_q} = -2.13 \ sec$$

The experimental method of measuring C_{M_q} is discussed in Appendix B.

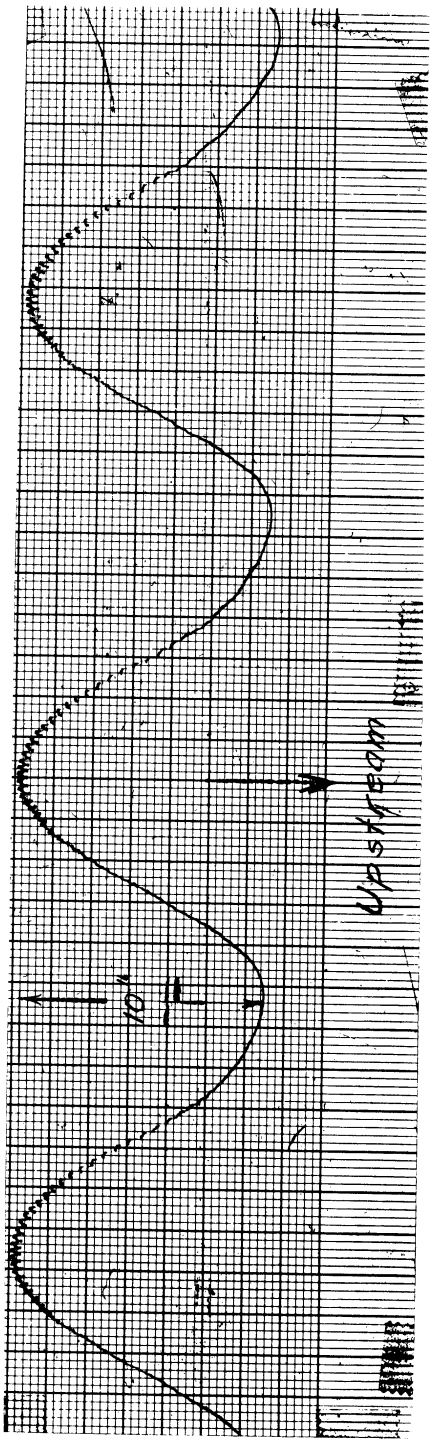

Figure 18. Bump Position vs. Time.

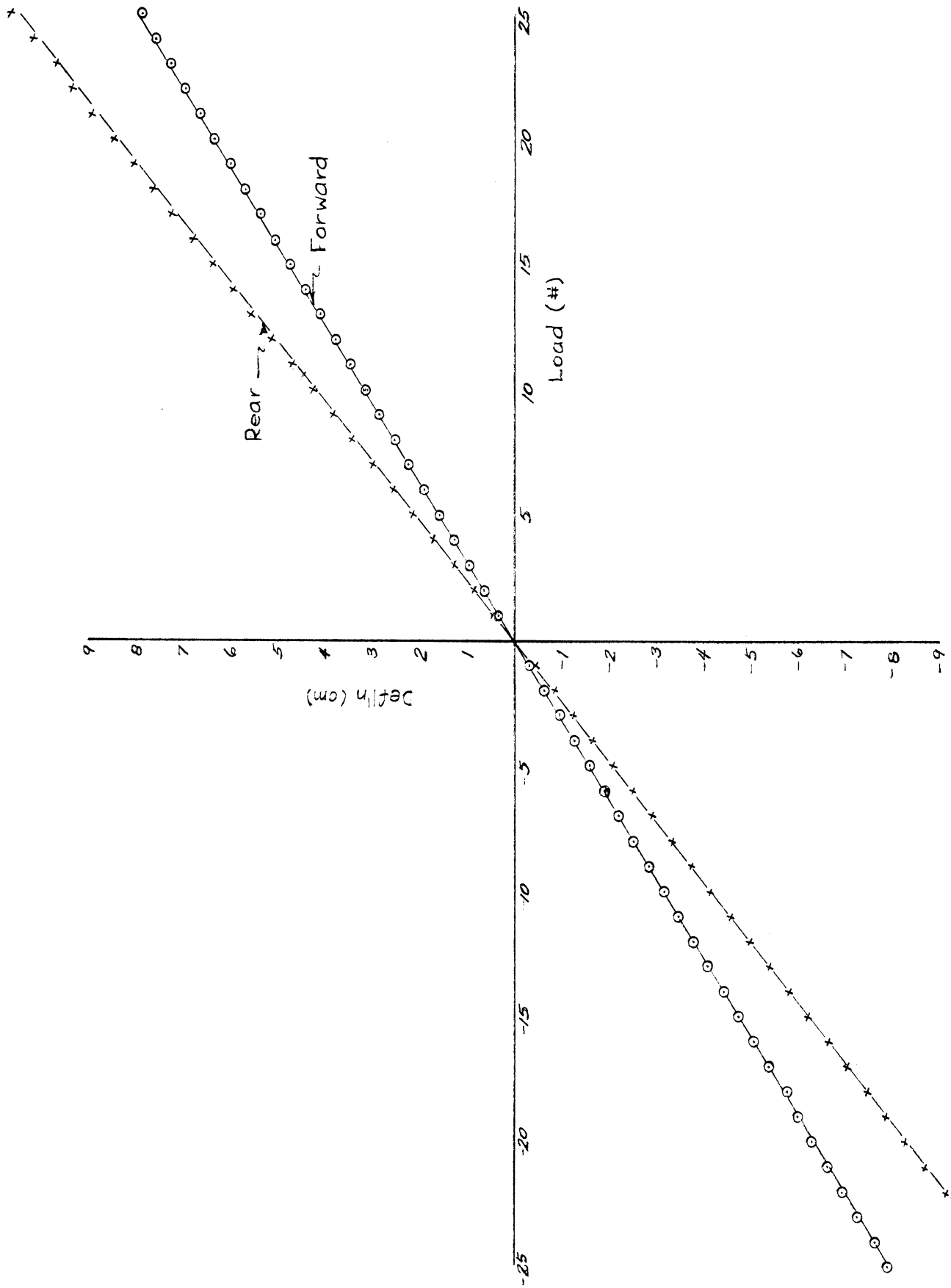

Figure 19. Fixed Mount Calibration Curves.

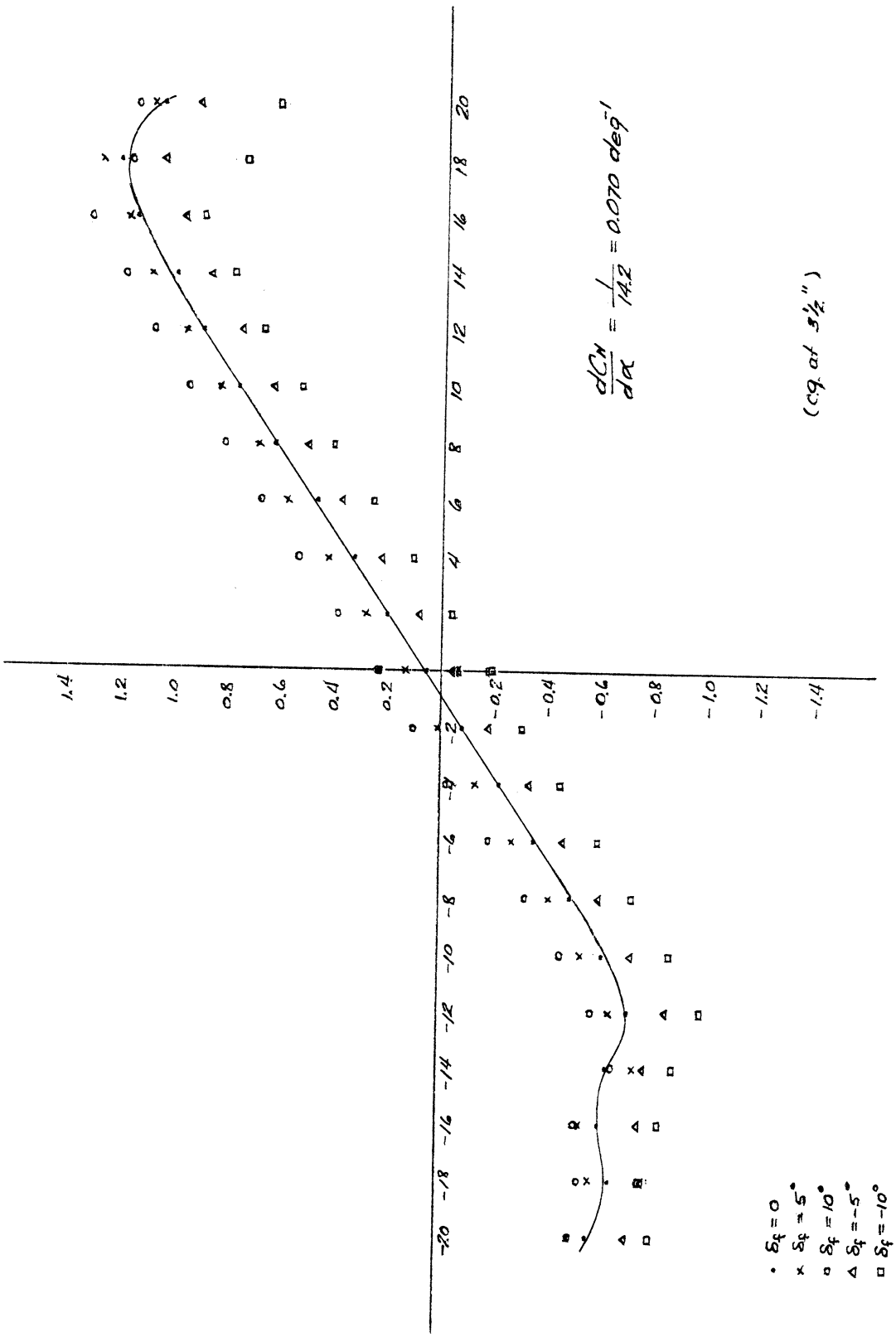

Figure 20. C_n vs. α for Various δ_f.

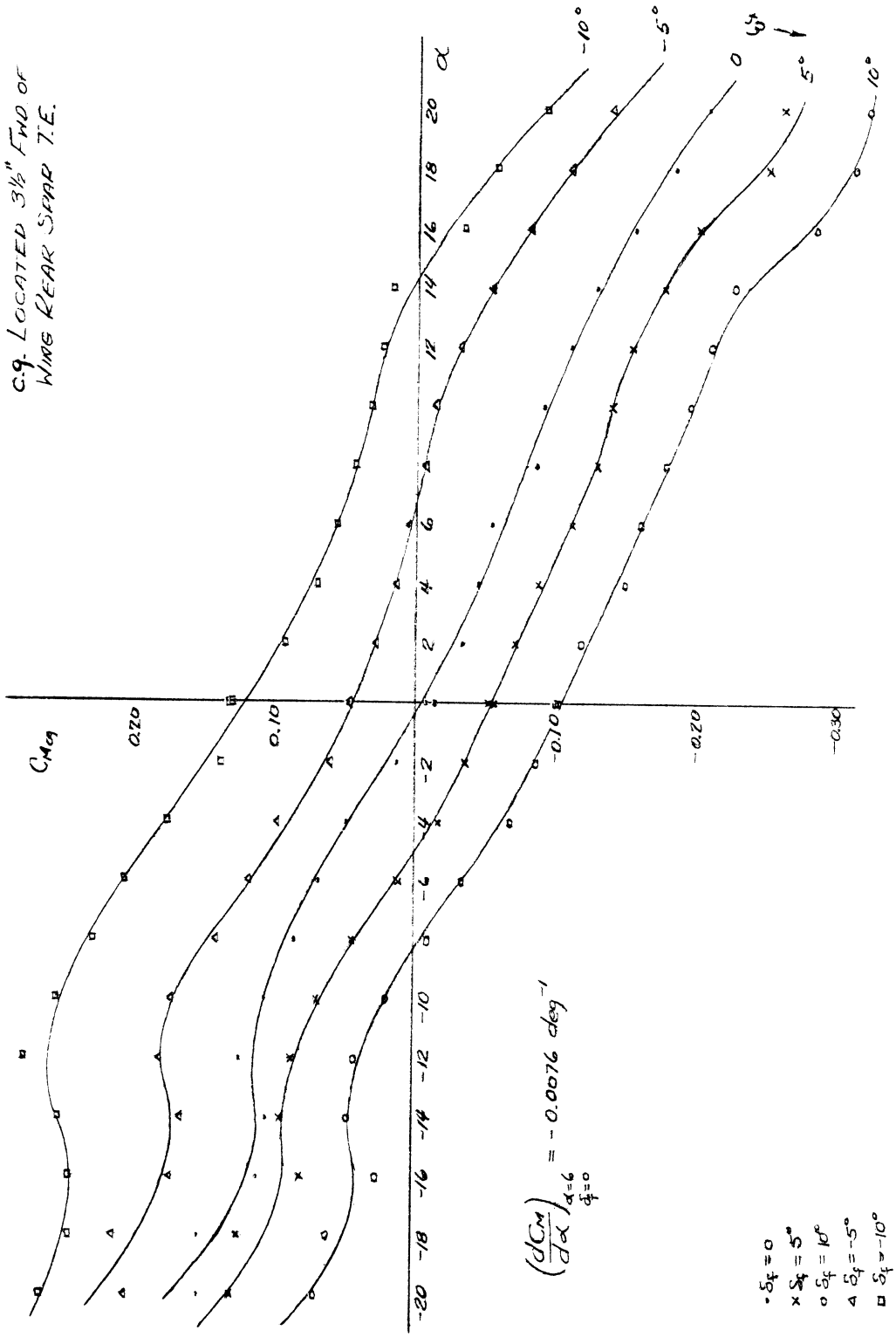

Figure 21. $C_{Mc.g.}$ vs. α for Various δ_f.

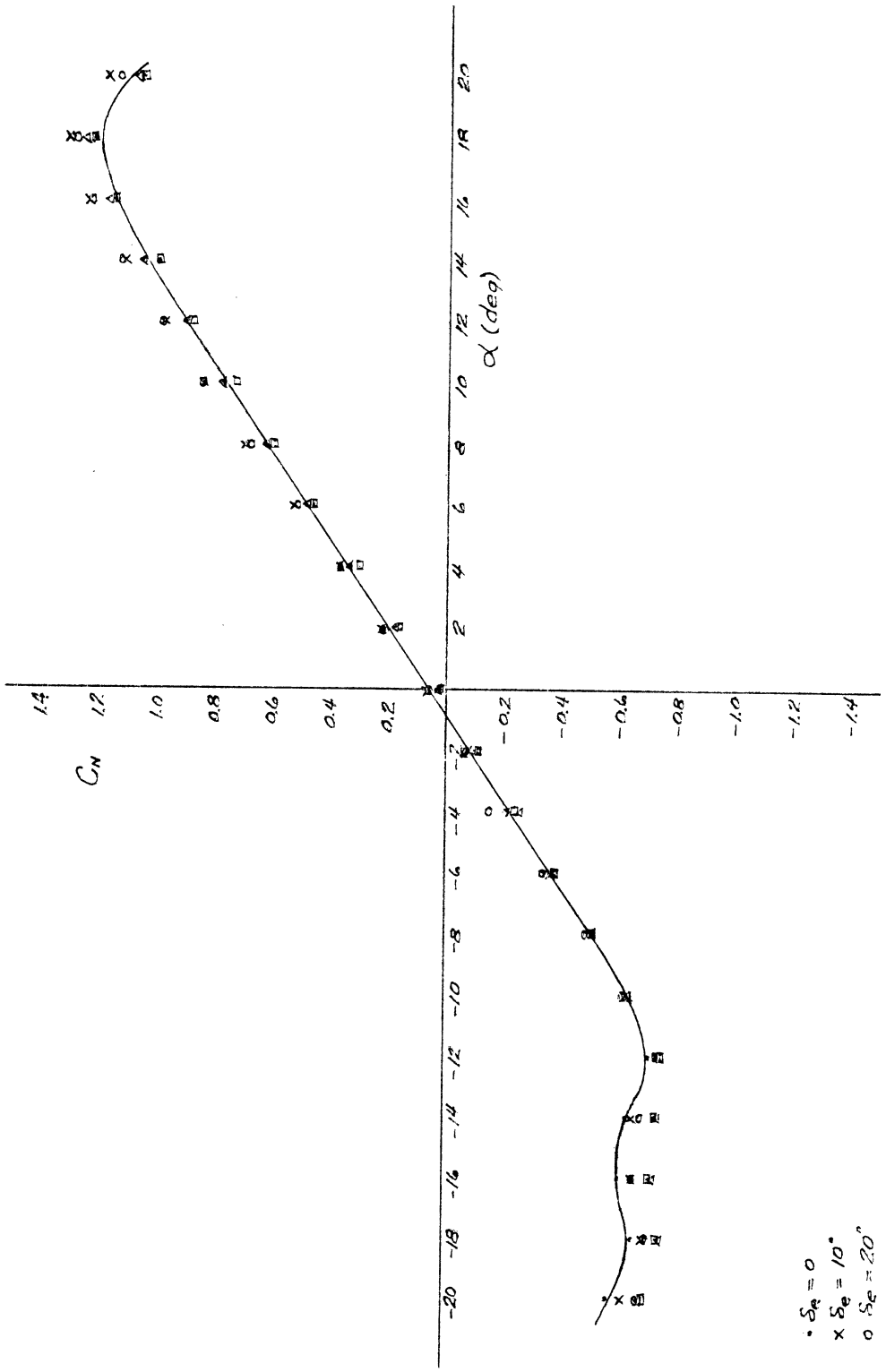

Figure 22. C_N vs. α for Various δ_e.

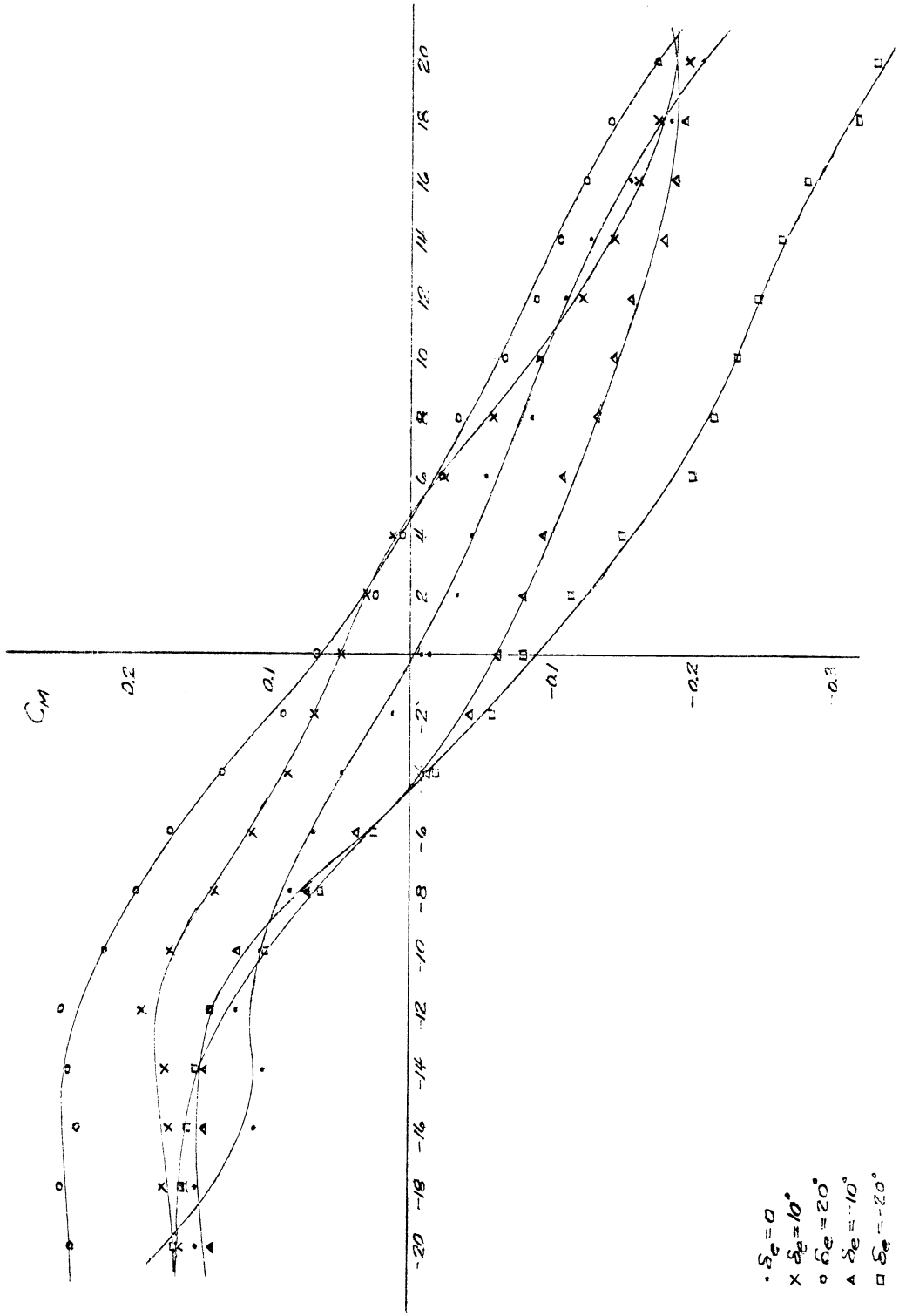

Figure 23. $C_{Mc.g.}$ vs. α for Various δ_e.

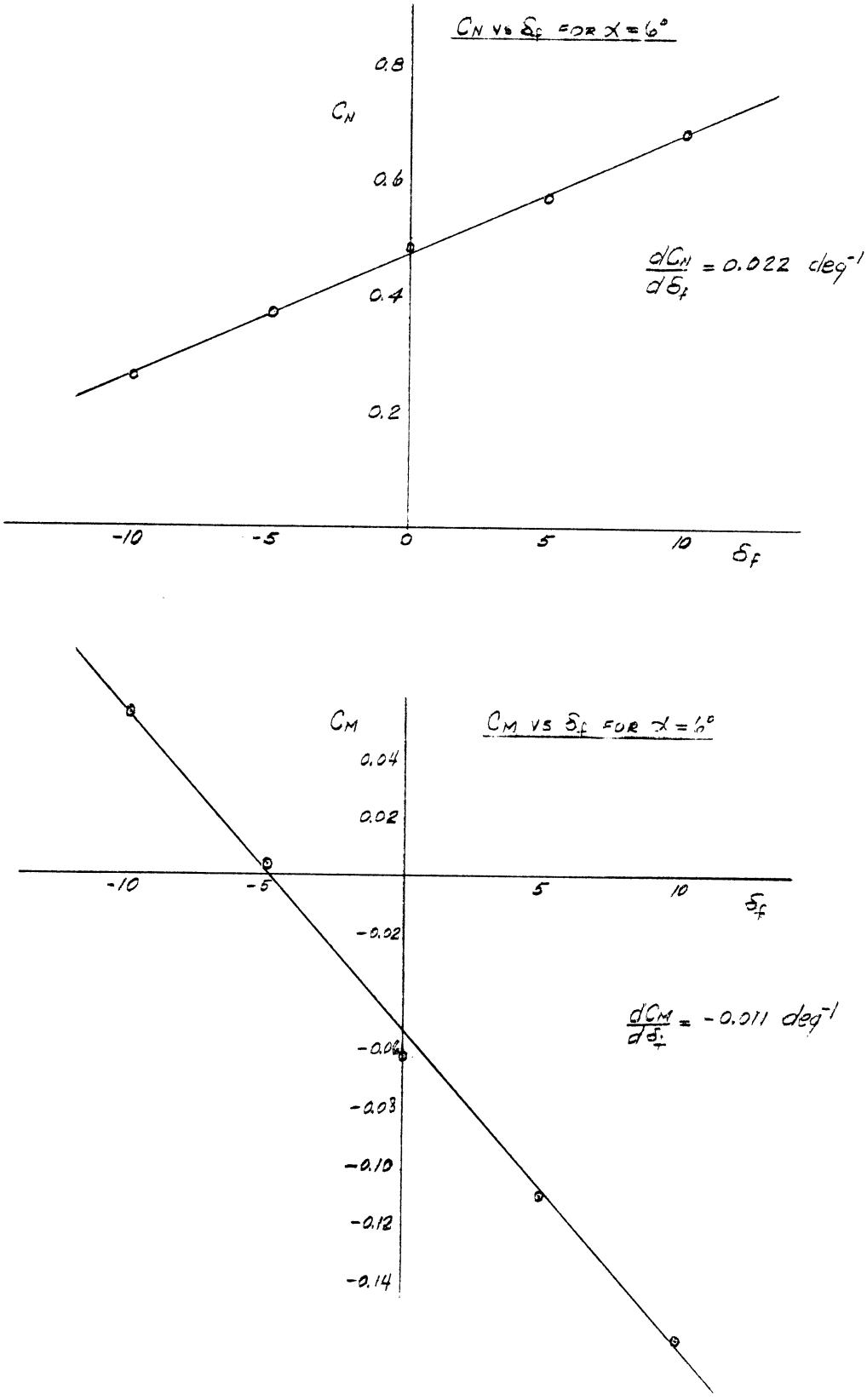

Figure 24. C_n and $C_{Mc.g.}$ vs. δ_f for $\alpha = 6°$.

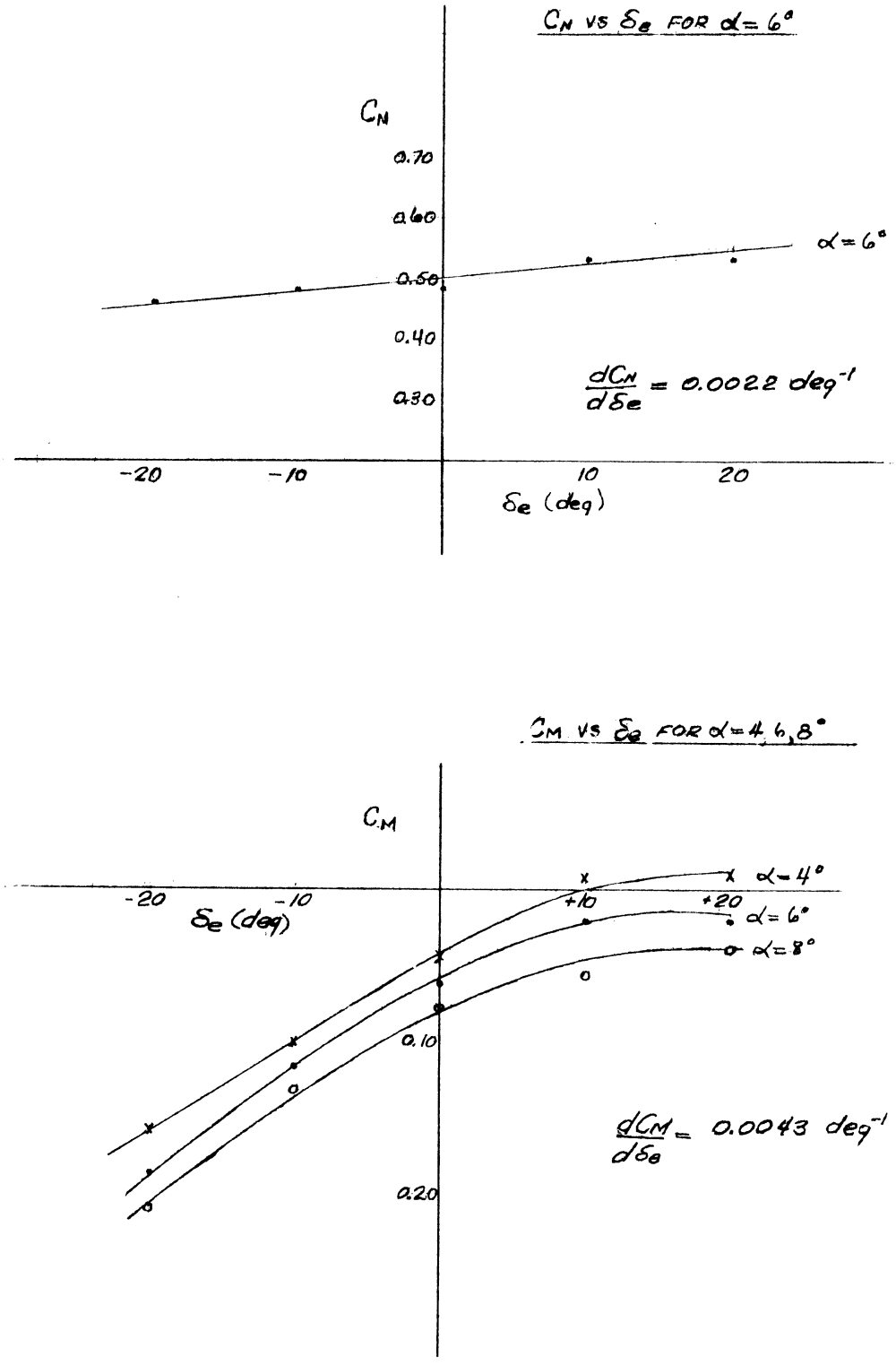

Figure 25. C_n and $C_{Mc.g.}$ vs. δ_e for α = 4, 6, 8°.

The phase angles measured between the control surface deflections and the forces thus generated are presented in Figure 26. The change in phase angle with frequency is small; hence, the unsteady aerodynamic effects appear to be negligible.

Conclusions and Recommendations

The tests performed have indicated the feasibility of performing dynamic wind tunnel tests of the type required for the design and evaluation of an automatic control system for the alleviation of airplane response to rough air. The method of sinusoidal gust generation appears to be satisfactory on the basis of no-flow tests. Since the perturbation aerodynamic forces on the bump are expected to be a small percentage of the dynamic and spring forces, the bump oscillation in the windstream is not expected to be significantly different than that obtained with no flow.

The strain gauge balance system has proven to be reliable and accurate, as indicated on the calibration curves. The servosystems for the operation of the control surfaces operate smoothly and supply sufficient torque to hold the controls at maximum deflection with maximum test airspeed. The instrumentation used to obtain the data for determination of the pitch damping, as described in Appendix B, was adequate but subject to improvement. It is recommended that a method be devised of forcing the oscillation in pitch only, rather than in pitch and yaw. It is also recommended that the pen-ink recording system be replaced by a reflected light or a photographic system. Results from the pilot-tests on the dynamic suspension system indicate that such a support is feasible, but it also should be improved. The necessary improvements can probably be obtained by using a movable post of extruded, rectangular aluminum tubing which is laterally constrained by bearing-mounted rollers. The results of the controls input tests justify the assumption that unsteady aerodynamic effects are negligible.

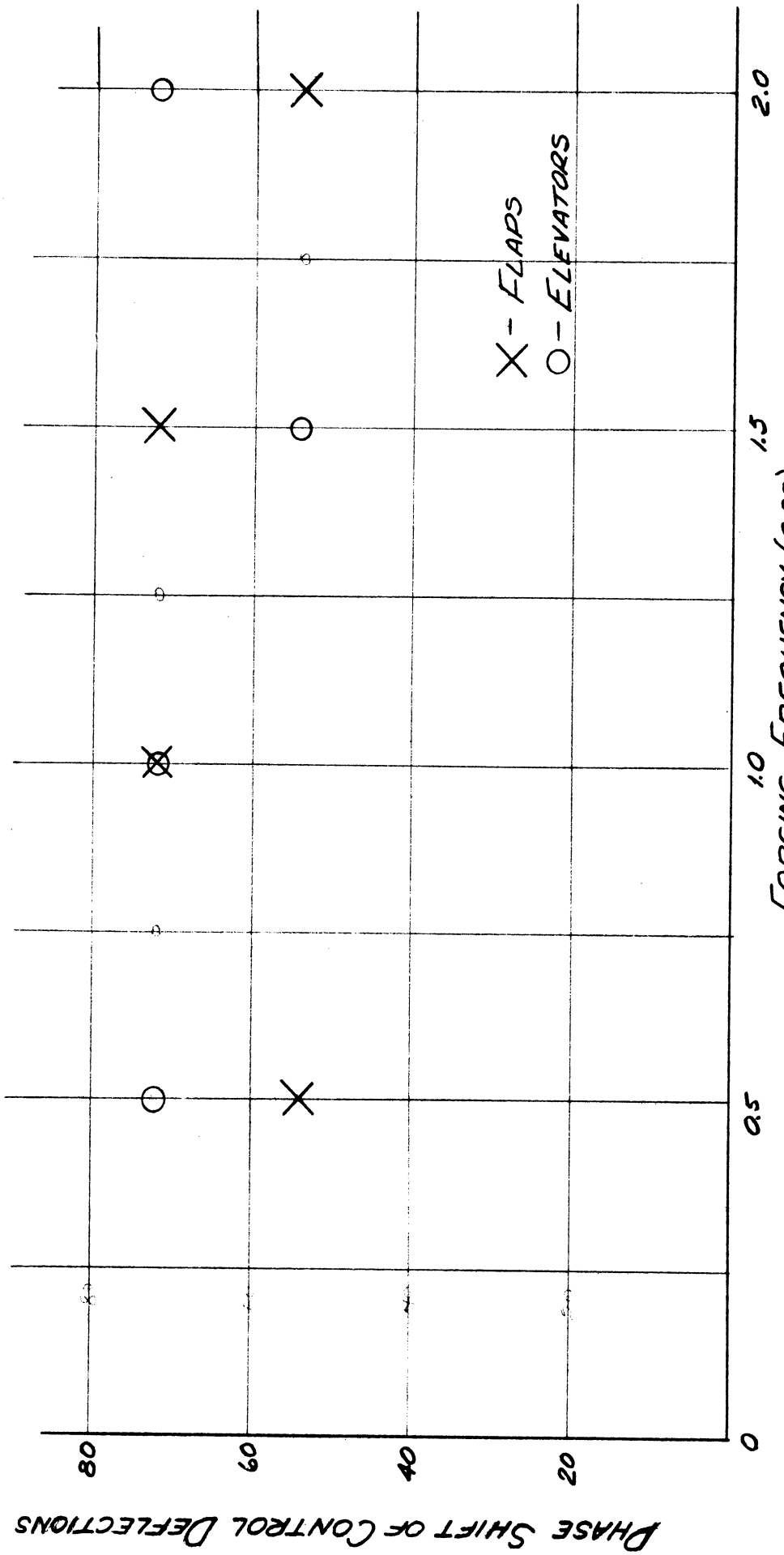

Figure 26. Controls Phase Shift Variation with Forcing Frequency.

APPENDIX A

Estimate of Gust Input

The airplane is trimmed in the non-uniform stream associated with bump position ℓ_o as shown in Figure A-1. The perturbation angle of attack at any station ξ is given by

$$\delta\alpha = (\alpha_2 - \alpha_o)\sin\omega t$$

$$\alpha_1 = m_1 \xi/c + a_1$$

$$\alpha_2 = m_2 \xi/c + a_2$$

$$\alpha_o = \frac{\alpha_1 + \alpha_2}{2} = \left(\frac{m_1 + m_2}{2}\right)\xi/c + \frac{a_1 + a_2}{2}$$

$$\delta\alpha = \left[\left(\frac{m_2 + m_1}{2}\right)\xi/c + \left(\frac{a_2 - a_1}{2}\right)\right]\sin\omega t$$

The quasi-steady lift due to the non-uniform distribution of angle of attack is computed from the formulae[42] below:

$$\Gamma_Q = -2\pi b \sum_{n=1}^{\infty} E_n$$

$$\bar{u} = \frac{1}{2}\sum_{n=1}^{\infty} E_n\left[\frac{1 - \cos n\theta}{\sin\theta}\right] \qquad x = 2b\cos\theta$$

$$E_n = \frac{2}{\pi}\int_{-\pi}^{\pi} g(x)\sin n\theta \sin\theta\, d\theta$$

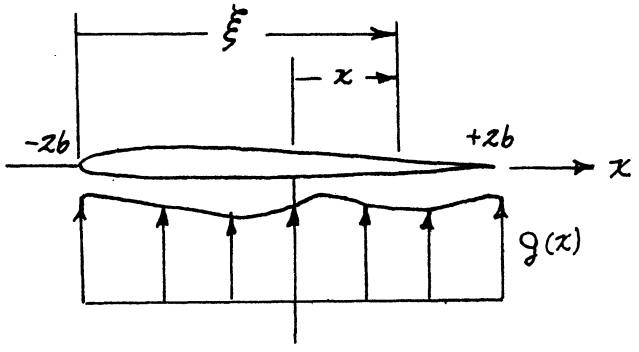

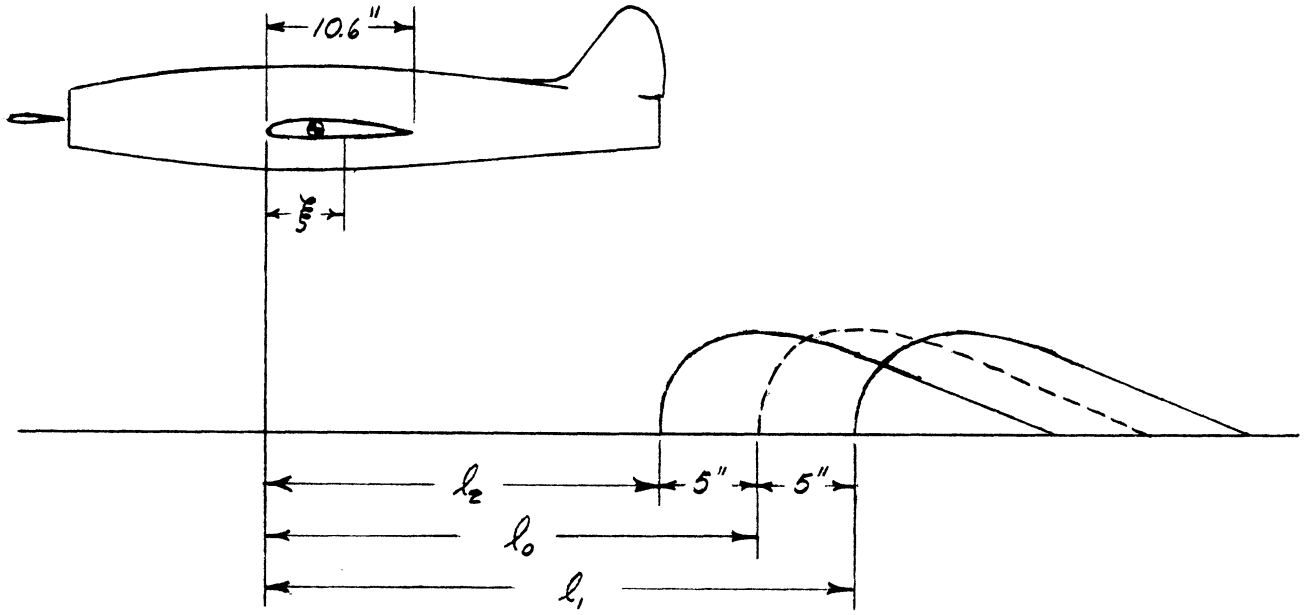

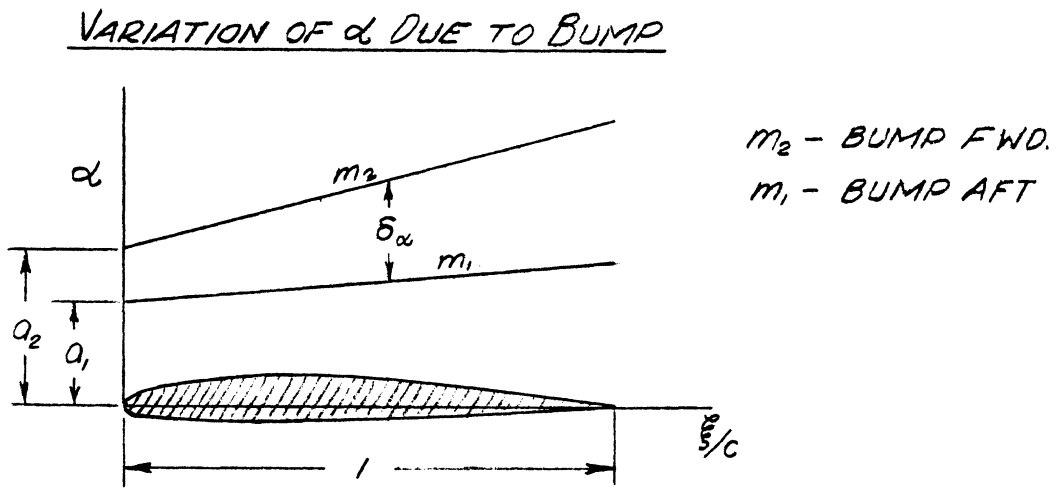

Figure A-1. Model-Bump Orientation and Variation of α Due to Bump.

$$\xi = x + 2b$$

$$\xi/c = \frac{1}{2}(\cos\theta + 1)$$

$$q = V_\infty \left[\frac{m_2 - m_1}{4}(\cos\theta + 1) + \frac{a_2 - a_1}{2}\right] \sin\omega t$$

$$E_n = \frac{2V_\infty}{\pi} \sin\omega t \int_{-\pi}^{\pi} \left[\left(\frac{m_2 - m_1}{4}\right)(\cos\theta + 1) + \left(\frac{a_2 - a_1}{2}\right)\right] \sin n\theta \sin\theta \, d\theta$$

$$E_n = \frac{2V_\infty}{\pi} \sin\omega t \int_{-\pi}^{\pi} \left[\left(\frac{m_2 - m_1}{4}\right)\left(\frac{\sin 2\theta}{2}\right)\sin n\theta + \left(\frac{m_2 - m_1}{4}\right)\sin n\theta \sin\theta + \left(\frac{a_2 - a_1}{2}\right)\sin n\theta \sin\theta\right] d\theta$$

$$E_1 = V_\infty \left[\left(\frac{m_2 - m_1}{2}\right) + (a_2 - a_1)\right] \sin\omega t$$

$$E_2 = V_\infty \left[\frac{m_2 - m_1}{4}\right] \sin\omega t$$

$$\Gamma_Q = -2\pi b V_\infty \left[\frac{3}{4}(m_2 - m_1) + (a_2 - a_1)\right] \sin\omega t$$

$$L = 2\pi b \rho V_\infty^2 \left[\frac{3}{4}(m_2 - m_1) + (a_2 - a_1)\right] \sin\omega t$$

$$c_\ell = \frac{L}{q 4b} = \pi \left[\frac{3}{4}(m_2 - m_1) + (a_2 - a_1)\right] \sin\omega t$$

The equivalent uniform angle of attack is given by

$$\delta\alpha_{eq} = \left[\frac{3}{4}\left(\frac{m_2 - m_1}{2}\right) + \left(\frac{a_2 - a_1}{2}\right)\right] \sin\omega t$$

The gust input, therefore, is equivalent to a uniform sinusoidal updraft as shown in Figure A-2.

A plot of angle of attack distribution in the tunnel at various points upstream of the bump is shown in Figure A-3. The position of the airfoil in the stream with the bump in its forward position (ℓ_2 in Figure A-1) is indicated between points A and B. With the bump rearward, the airfoil

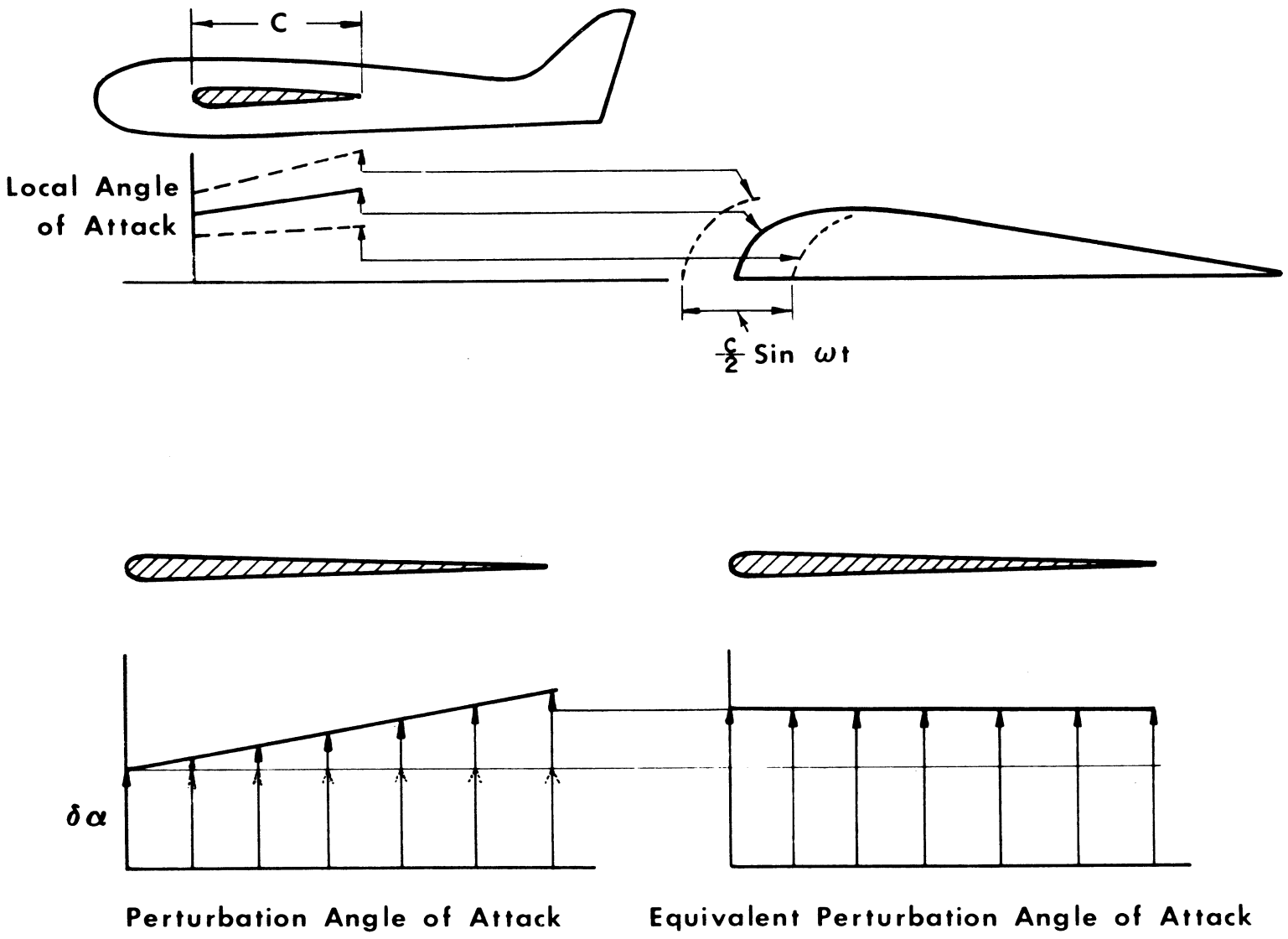

Figure A-2. Airplane in Non-uniform Stream.

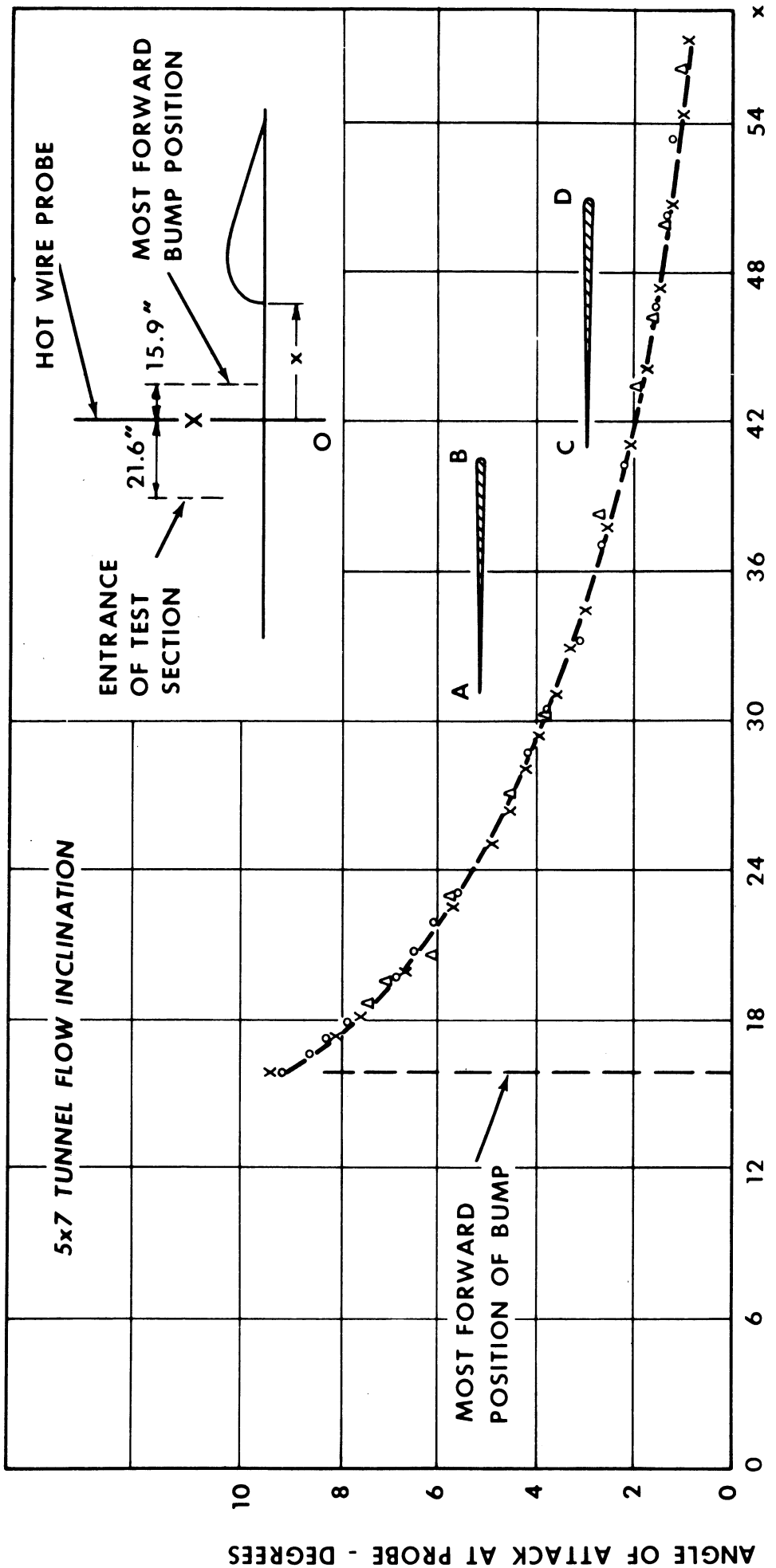

Figure A-3. 5 x 7 Tunnel Flow Inclination.

between C and D. We have, therefore:

$$\alpha_1' = 1.14^\circ \qquad m_1 = 0.86$$

$$\alpha_2 = 2^\circ \qquad m_2 = 1.56$$

and

$$\delta_{eff} = 0.0121 \sin \omega t$$

APPENDIX B

Determination of Pitch Damping

The method used in the evaluation of the pitch damping coefficient is based upon that suggested by Durant[42]. The equation of motion is written for a single-degree-of-freedom forced oscillation with and without wind-tunnel flow. Resonance conditions are obtained and the necessary physical data are measured to calculate the pitch damping coefficient. A detailed discussion of the method used is given below.

The model was mounted in the wind tunnel as shown in Figure B-2 on the dynamic suspension system near the center of the test section. The mount was clamped in position to prevent plunging motion; hence, the model was free to move in pitch only. The forcing function was applied to the model through spring k_3 by displacing the spring with a motor-driven eccentric. The speed of the eccentric rotation was controlled by controlling the input voltage to the motor with a variac. The equation of the motion of the model was written as follows:

$$I_{yy}\ddot{\theta} + (\mu_o + \mu_1)\dot{\theta} - (M_\alpha - k_1 l_1^2 - k_3 l_2^2)\theta = k_3 l_2 h_o \cos \omega t$$

where μ_o = aerodynamic damping

μ_1 = friction damping

This was rewritten as:

$$I_{yy}\ddot{\theta} + \mu\dot{\theta} + k\theta = f_o e^{i\omega t}$$

where $\mu = \mu_o + \mu_1$ (wind on)

$\mu = \mu_1$ (wind off)

$$k = -(M_\alpha - k_1 l_1^2 - k_3 l_2^2)$$

$$f_o = k_3 l_2 h_o$$

At resonance, the inertia and spring forces cancel, and

$$\mu = \frac{-i f_o}{\omega_n \theta_{max}}$$

or

$$|\mu| = \frac{k_3 l_2 h_o}{\omega_n \theta_{max}}$$

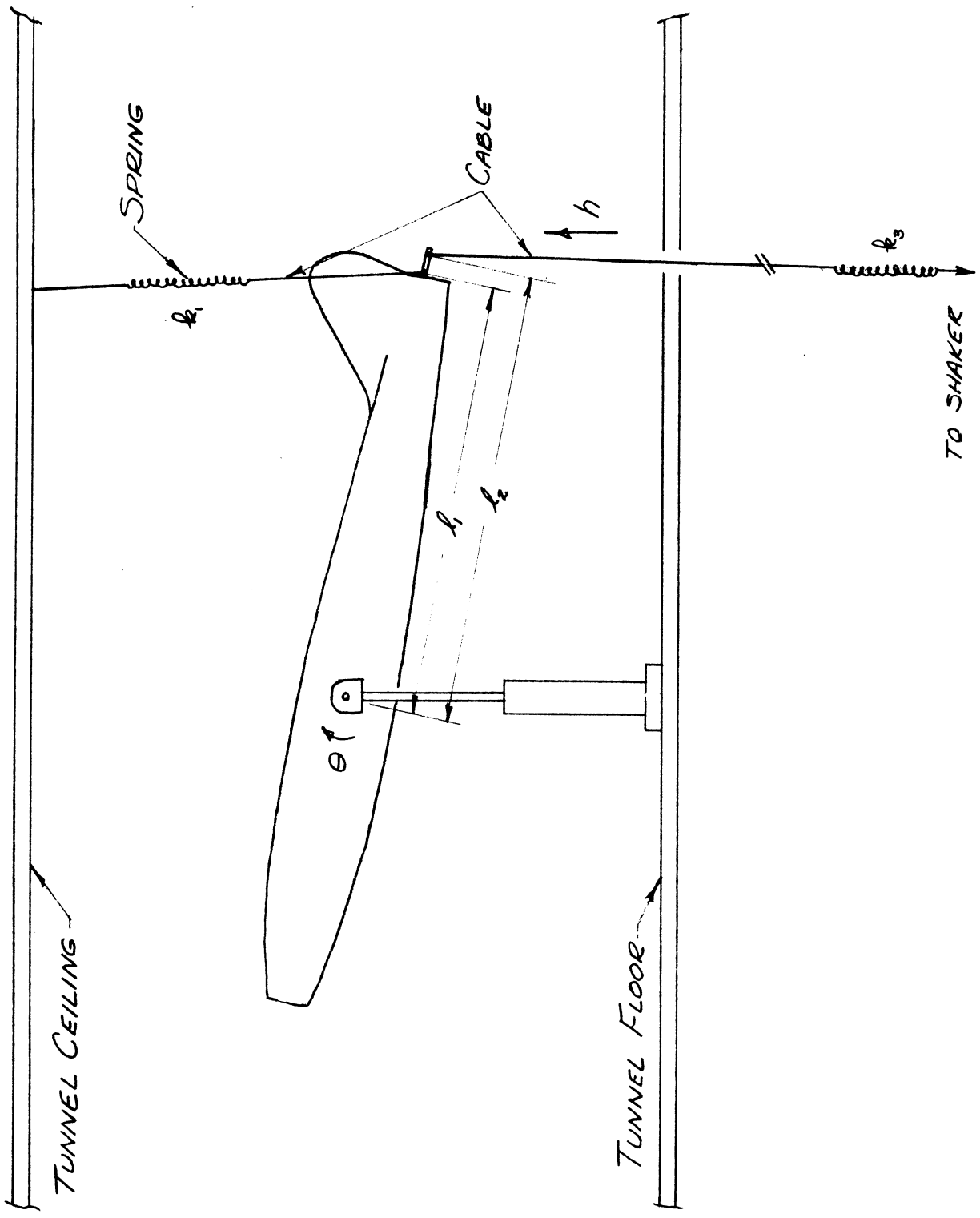

Figure B-1. Model Mounting for Damping Tests.

Assuming only the wings and tail to contribute to μ, Durand shows that:

$$M_q = M_q^\circ + M_q' = \frac{(\mu_o + M_q^\circ \, d\varepsilon/d\alpha)}{1 + d\varepsilon/d\alpha}$$

where M_q° - pitching moment due to wings

M_q' - pitching moment due to tail

$$\mu_o = \mu - \mu_1$$

The upwash at the forward mounted tail was assumed negligible (i.e., $d\varepsilon/d\alpha = 0$); hence,

$$|M_q| = |\mu| - |\mu_1|$$

The damping coefficient was then formulated as

$$C_{M_q} = \frac{-|M_q|}{\rho \frac{V_\infty}{4} S c^2}$$

The damping coefficients, $|\mu|$ and $|\mu_1|$, were calculated from measured values of k_s, l_t, and h_o and experimentally determined values of ω_n and θ_{max}.

The values of ω_n and θ_{max} were obtained by recording the vertical displacement of the downstream end of the model using an ink pen from a Brown recorder attached to the cable as shown in Figure B-2. The modulus of the ratio θ_o/θ_i, was then calculated and plotted versus forcing frequency, as shown in Figures B-3 and B-4. The natural frequency was taken to be the value of the frequency at the indicated resonance. The calculations for the determination of C_{M_q} are shown below.

Calculations of $|\mu_1|$ (wind off):

$$|\mu_1| = \frac{k_s l_t h_o}{\omega_n \theta_{max}}$$

$k_s = 0.248$ #/in

$h_o = 0.20$ in

$l_t = 38$ in

From Figure B-3, $\omega_n = 8.5$ rad/sec

From recording, $\left|\frac{\theta_o}{\theta_i}\right|_{max} \simeq 42$

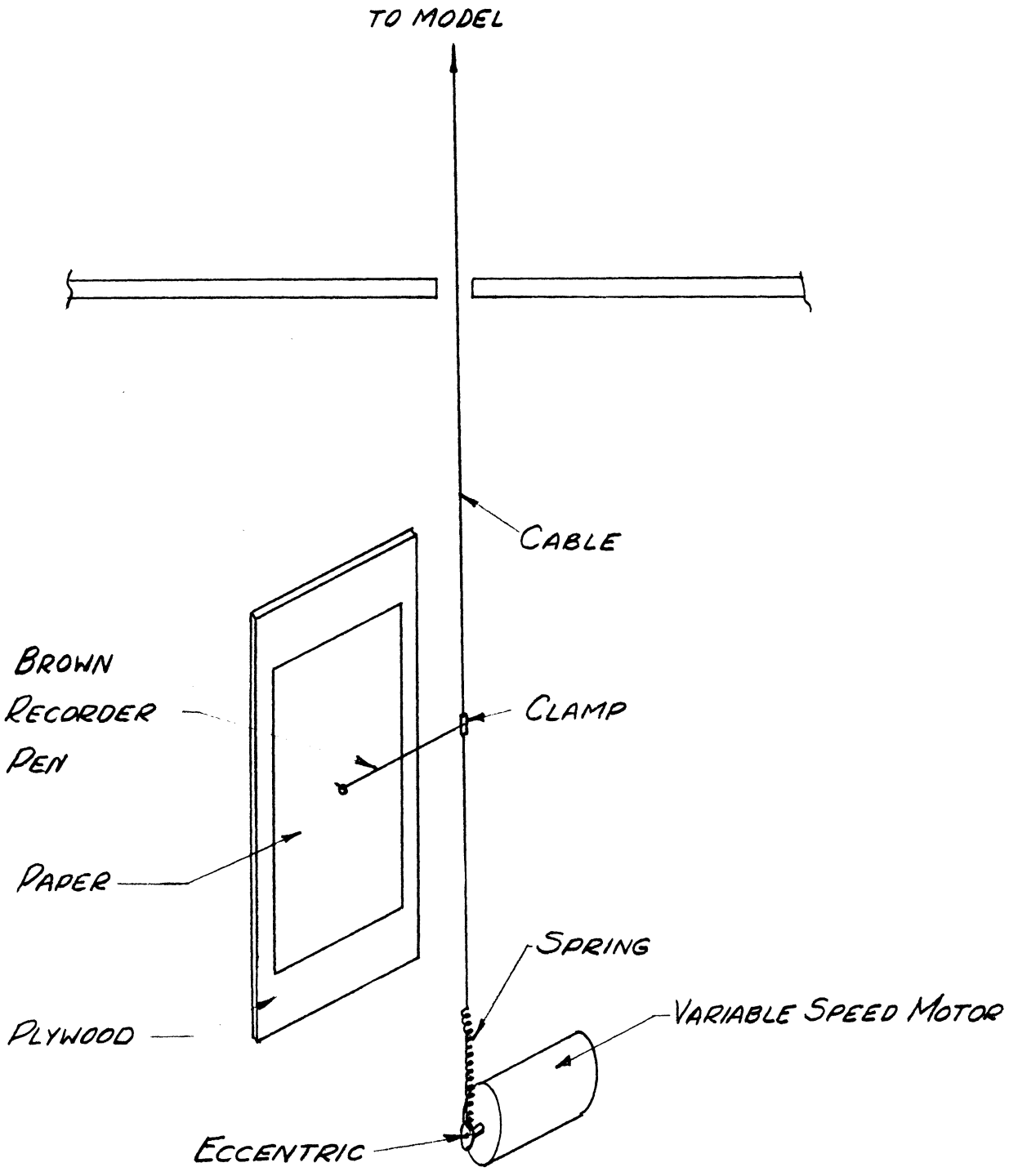

Figure B-2. Instrumentation for Damping Tests.

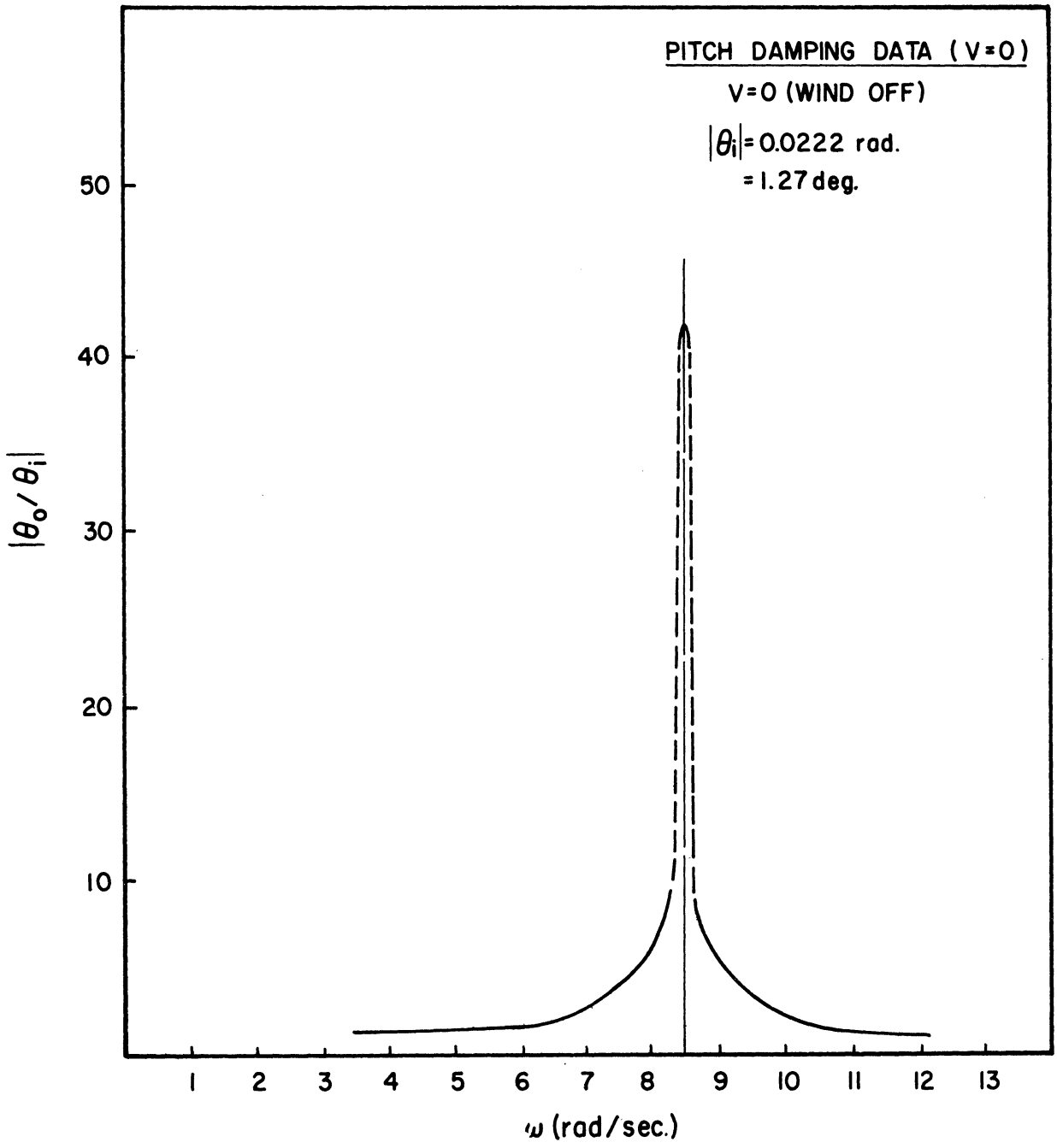

Figure B-3. Pitch Damping Data (V = 0).

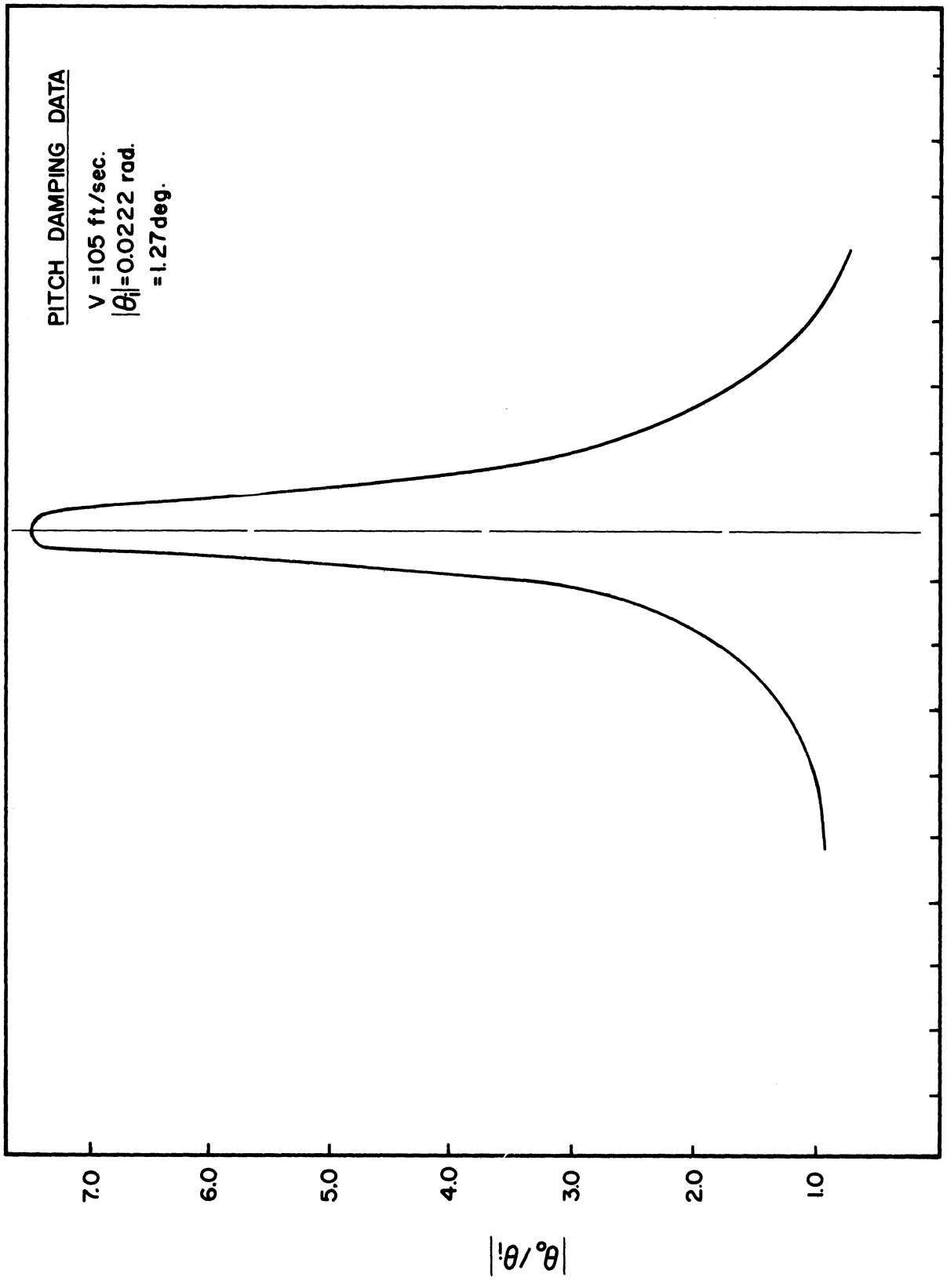

Figure B-4. Pitch Damping Data.

And $\theta_i = \frac{h_o}{l_z} = 0.0052$ rad.

Hence, $\theta_{max} = (42)\ (0.0052) = 0.22$ rad.

Therefore, $|\mu_i| = \frac{(0.248)\ (38)\ (0.20)}{(8.5)\ (0.22)} = \frac{1.88}{1.87}$

$|\mu_i| \cong 1.0$ in$^{\#}$ sec

Calculation of $|\mu|$ (wind on):

$$|\mu| = \frac{k_z l_z h_o}{\omega_n \theta_{max}}$$

From Figure B-4

$$\omega_n = 9.75 \text{ rad/sec}$$

From recording,

$$\left|\frac{\theta_{max}}{\theta_i}\right| = 7.5$$

Hence, $\theta_{max} = (7.5)\ (0.0052) = 0.039$ rad.

Therefore, $|\mu| = \frac{(0.248)\ (38)\ (0.20)}{(9.75)\ (0.039)}$

$|\mu| = 4.97$ in$^{\#}$ sec

Calculation of C_{M_q}:

$|M_q| = |\mu| - |\mu_i|$

$= 4.97 - 1.00 = 3.97$ in$^{\#}$ sec

$|M_q| = 0.33$ ft$^{\#}$ sec

$V = \sqrt{\frac{2\bar{q}}{\rho}}$ where $\bar{q} = 2.300$ "Hg at 75°F

Since $T_Q = 75°F$, the correction to $P_b = -0.13$ "Hg. Hence, the corrected barometric pressure = 28.90 "Hg, and the test-section temperature (T_t) = 460 + 87 = 547°R.

Hence, $\rho = \rho_o \left(\frac{T_o}{T}\right)\left(\frac{p_c}{p_o}\right) = 2.378 \cdot 10^{-3} \left(\frac{519}{547}\right)\left(\frac{28.90}{29.92}\right)$

$$\rho = 2.178 \cdot 10^{-3} \text{ slug/ft}^3$$

Also, $\bar{q} = (2.300)\,(0.0361)\,(144) = 11.95 \text{ \#/ft}^2$

Therefore, the wind tunnel speed was

$$V_\infty = \sqrt{\frac{2(11.95)10^4}{2178}} = 104.8 \text{ ft/sec}$$

Then $$C_{M_q} = \frac{-4(0.33)}{\rho V_\infty S c^2} = \frac{-4(0.33)}{(2.31)\,(104)\,(0.337)\,(0.78)}$$

$$C_{M_q} = -2.13$$

REFERENCES

1.) Shufflebarger, C.C.: Tests of a Gust Alleviating Wing in the Gust Tunnel. NACA TN802; April, 1941.

2.) Reisert, T.D.: Gust Tunnel Investigation of a Flexible-Wing Model with Semi-Chord Line Swept Back 45°. NACA TN 1959; October, 1949.

3.) Hirsch, Rene: Recherches Theoretiques et Experimentales Sur les Moyers de Soustraire un Avion aux Accelerations que Reurent Engendrer les Perturbations Atmospheriques. Publications Scientifiques et Techniques du Ministere de l'Air. No. 138, Paris, 1938.

4.) Dynamic Analysis of a Gust Load Alleviation System. Douglas Aircraft Report SM-13699; January, 1950.

5.) Schetzer, J.D., Howe, R.M., et al: Dynamics of Flight. Notes for an Intensive Short Course at the University of Michigan.

6.) Tobak, M.: On the Use of the Indicial Function Concept in the Analysis of Unsteady Motions of Wings and Wing-Tail combinations. NACA Report 1188, 1954.

7.) Blishpinghoff, R. L., Ashley, H., and Halfman, R.L.: Aeroelasticity. Addison-Wesley Publishing Co., Inc. (Cambridge), 1955.

8.) Sears, W.R., and von Karman, T.: Airfoil Theory for Non-Uniform Motion. Journal of the Aeronautical Sciences; May, 1938.

9.) Sears, W.R., and Sparks, .: Some Aspects of Non-Stationary Airfoil Theory and Its Practical Application. Journal of the Aeronautical Sciences; January, 1941.

10.) Richardson, A. S., Jr.: Theoretical and Experimental Investigation of Random Gust Loads. Part II - Theoretical Formulation of Atmospheric Gust Response Problem. NACA TN 3379; May, 1957.

11.) Laning, J.H., Jr., and Battin, R.H.: Random Processes in Automatic Control. Mc-Graw - Hill Book Co., Inc., 1956.

12.) Chilton, R. G.: Some Measurements of Atmospheric Turbulence Obtained from Flow-Direction Vanes Mounted on an Airplane. NACA TN3313; November, 1954.

13.) Phillips, W.H., and Kraft, C.C.: Theoretical Study of Some Methods of Increasing the Smoothness of Flight Through Rough Air. NACA TN 2416; July, 1951.

14.) Tobak, M.: On the Minimization of Airplane Responses to Random Gusts. NACA TN3290; October, 1957.

15.) Boucher, R.W., and Kraft, C.C.: Analysis of a Vane Controlled Gust Alleviation System. NACA TN 3597; April, 1956.

16.) Croom, D.R., and Shufflebarger, C.C.: An Investigation of Forward Located Fixed Spoilers and Deflectors as Gust Alleviators on an Unswept Wing Model. NACA TN 3705; June, 1956.

17.) Heaslet, M.A., and Lomax, H.: Two-Dimensional Unsteady Lift Problems in Supersonic Flight. NACA Report 945, 1949.

18.) Lomax, H., Heaslet, M.A., Fuller, F.B., and Sluder, L.: Two- and Three-Dimensional Unsteady Lift Problems in High-Speed Flight. NACA Report 1077, 1952.

19.) Donely, P., and Shufflebarger, C.C.: Tests of a Gust Alleviating Flap in the Gust Tunnel. NACA TN745; January, 1940.

20.) Liepmann, H.W.: On the Application of Statistical Concepts to the Buffeting Problem. Journal of the Aeronautical Sciences; December, 1952.

21.) Liepmann, H.W.: Extension of the Statistical Approach to Buffeting and Gust Response of Wings of Finite Span. Journal of the Aeronautical Sciences; March, 1955.

22.) Press, H., and Mazelsky, B.: A Study of the Application of Power-Spectral Methods of Generalized Harmonic Analysis to Gust Loads on Airplanes. NACA Report 1172; 1954.

23.) Press, H., and Houbolt, J.C.: Some Applications of Generalized Harmonic Analysis to Gust Loads on Airplanes. Journal of the Aeronautical Sciences; January, 1955.

24.) Tukey, J.W.: The Sampling Theory of Power Spectrum Estimates. Symposium on Applications of Autocorrelation Analysis to Physical Problems (Woods Hole, Mass., June, 1949) Office of Naval Research, May, 1950.

25.) Diederich, F.W., and Drischler, J.A.: Effect of Spanwise Variations in Gust Intensity on the Lift Due to Atmospheric Turbulence. NACA TN 3920; April, 1957.

26.) Etkin, B.: A Theory of the Response of Airplanes to Random Atmospheric Turbulence. Journal of the Aeronautical Sciences; July, 1959.

27.) Ribner, H.S.: Spectral Theory of Buffeting and Gust Response. Journal of the Aeronautical Sciences; December, 1956.

28.) Weiner, N.: Extrapolation, Interpolation, and Smoothing of Stationary Time Series, with Engineering Applications. John Wiley and Sons, Inc., New York, 1949.

29.) Kraft, C.C.: Initial Results of a Flight Investigation of a Gust Alleviation System. NACA TN 3612; April, 1956.

30.) Cooney, T.V. and Schott, R.L.: Initial Results of a Flight Investigation of the Wing and Tail Loads on an Airplane Equipped with a Vane Controlled Gust Alleviation System. NACA TN 3746; September, 1956.

31.) Lamson, P.: Measurements of Lift Fluctuations Due to Turbulence. NACA TN 3880; March, 1957.

32.) Mickleboro, H.C.: Evaluation of a Fixed Spoiler as a Gust Alleviation. NACA TN 1753; November, 1948.

33.) Clementson, G.C.: An Investigation of the Power Spectral Density of Atmospheric Turbulence. Ph. D. Thesis, M.I.T., 1950.

34.) Hakkinen, R.J., and Richardson, A.S.: Theoretical and Experimental Investigation of Random Gust Loads. Part I. TN 3878; May, 1957.

35.) Garby, L.C., Kuethe, A.M., and Schetzer, J.D.: The Generation of Gusts in a Wind Tunnel and Measurement of Unsteady Lift on an Airfoil. WADC TR 57-401; June, 1957.

36.) Smith, F.B.: Analog Equipment for Processing Randomly Fluctuating Data. Institute of Aeronautical Sciences Review; May, 1955.

37.) Wade, W.F., and Thom, N.R.: Generation and Investigation of Sinusoidal Gusts. Masters Degree Thesis, University of Michigan, 1958.

38.) Kraft, C.C., and Assadourian, A.: Experimental Study of an Angle-of-Attack Vane Mounted Ahead of the Nose of an Airplane for Use as a Sensing Device for an Acceleration Alleviator. NACA TN2415; July, 1951.

39.) Press, H., Meadows, M.T., and Hadlock, I.: A Reevaluation of Data on Atmospheric Turbulence and Airplane Gust Loads for Application in Spectral Calculations. NACA TR 1272; March, 1956.

40.) Rice, S.O.: Mathematical Analysis of Random Noise. Parts I and II. Bell System Tech. Journal, vol. XXIII, no. 3, July, 1944; Parts III and IV, vol. XXIV, no. 1, January, 1945.

41.) Schetzer, J.D., and Lemm, R.G.: Stability of Airborne Platforms in Rough Weather. Project 2144-093 Z-1022 Interim Report; January, 1958. University of Michigan Engineering Research Institute.

42.) Durand, W.F.: Aerodynamic Theory. Volume V, 1943.